

Intended for



Baltica-2 Wind Farm LLC  
(*Elektrownia Wiatrowa Baltica-2 Sp. z o.o.*)

Baltica-3 Wind Farm LLC  
(*Elektrownia Wiatrowa Baltica-3 Sp. z o.o.*)



ul. Mokotowska 49  
00-542 Warszawa  
Poland

Document type

**EIA Report**

Date

19.06.2022


Document number

Raport\_z\_modelowania\_Zal\_3\_EN\_A

# **ENVIRONMENTAL IMPACT ASSESSMENT REPORT ON THE CONNECTION INFRASTRUCTURE OF THE BALTICA-2 AND BALTICA-3 OFFSHORE WIND FARMS**

**APPENDIX 3 – MODELLING OF ELECTROMAGNETIC FIELD IN THE  
AREA OF THE RAIL BRIDGES CONNECTING THE PROJECTED  
BALTICA-2 AND BALTICA-3 LPSs WITH CHOZEWO PS AND THE  
CABLE BERM EVACUATING POWER FROM THE BALTICA OFFSHORE  
WIND FARM TO THESE LPSs**

Applicant            **Baltica-2 Wind Farm LLC**  
*(Elektrownia Wiatrowa Baltica-2 Sp. z o.o.)*             **baltica2** | by PGE & Ørsted  
**Baltica-3 Wind Farm LLC**  
*(Elektrownia Wiatrowa Baltica-3 Sp. z o.o.)*             **baltica3** | by PGE & Ørsted

Contractor            **MEWO S.A.**             **MEWO**  
SUBSEA SOLUTIONS  
**Maritime Institute of the Gdynia Maritime University**             **INSTYTUT MORSKI**  
**UNIWERSYTET MORSKI w GDYNI**

Subcontractors      **EKOMARK**             **EKOMARK**  
**ENGINEERING CONSULTING**            ENGINEERING CONSULTING  
**Consulting and Engineering Office**

## List of contents

- Abbreviations and definitions ..... 4
- 1 Introduction ..... 5
- 2 Justification to exclude LPS from the calculations of electromagnetic field distribution ..... 6
- 3 Theoretical foundations of computational methods ..... 8
- 4 Distribution of the electromagnetic field intensity in the vicinity of the designed cable berm ..... 9
  - 4.1 Technical parameters of the designed cable berm..... 9
  - 4.2 Assumptions for the calculation of the magnetic field distribution in the vicinity of the designed cable berm ..... 11
  - 4.3 The results of calculations of the magnetic field distribution in the vicinity of the designed cable berm ..... 12
  - 4.4 Interpretation of the computation results..... 19
- 5 The distribution of the electromagnetic field intensity in the vicinity of busbars..... 20
  - 5.1 Assumptions for the computation of the electric and magnetic field intensity distribution in the vicinity of busbars ..... 20
  - 5.2 The results of calculations of the electric and magnetic field distribution in the vicinity of busbars ..... 22
  - 5.3 Interpretation of the computation results..... 24
- 6 The distribution of the cumulative magnetic field intensity..... 25
  - 6.1 Assumptions for the calculation of the cumulative magnetic field distribution in the vicinity of the designed cable berm ..... 25
  - 6.2 The results of calculations of the magnetic field distribution in the vicinity of the designed common cable berm ..... 29
  - 6.3 Interpretation of the results of calculations of the cumulated magnetic field intensity in the vicinity of the cable berm..... 36
- 7 Literature..... 37
- 8 List of tables ..... 38
- 9 List of figures ..... 39

## Abbreviations and definitions

Baltica-2 or B-2	area accepted for construction purposes under the Decision of 16 April 2012 (MFW/4/12) granting a permit to construct and use artificial islands, installations, and equipment in Polish marine areas; the Baltica-2 area is the western part of the Baltica OWF
Baltica-3 or B-3	area accepted for construction purposes under the Decision of 16 April 2012 (MFW/5/12) granting a permit to construct and use artificial islands, installations, and equipment in Polish marine areas; the Baltica-3 area is the eastern part of the Baltica OWF
OSH	occupational safety and health
Baltica OWF CI	Connection Infrastructure of the Baltica-2 and Baltica-3 OWFs
LPS	land power station
Baltica OWF	an investment consisting in the implementation of the Baltica Offshore Wind Farm with a maximum capacity of 2550 MW located within the Baltica-2 area (western part) and the Baltica-3 area (eastern part), for which the Regional Director for Environmental Protection in Gdańsk issued a decision on environmental conditions on 24 January 2020 (no.: RDOŚ-Gd-WOO.4211.21.2017.MJ.PW.AJ.37);
TDP	Technological Description of the Project
EMF	electromagnetic field
Project	The investment consisting in the construction of an offshore wind farm in accordance with the permits to construct and use artificial islands, installations, and devices issued under the decisions dated 16 April 2012 no. MFW/4/12 and MFW/5/12, together with its onshore connection infrastructure and the impact zone ( <i>conf.</i> "Project" definition provided in the Contract)
PSE	Polskie Sieci Elektroenergetyczne S.A.
PSZW	Permit to construct and use of artificial islands, installations and devices issued for offshore wind farms
EIA Report	Environmental Impact Assessment Report
RAV	Rational Alternative Variant
PS	Power Station
APV	Variant Proposed by the Applicant

**Author:**

Marek Szuba

**Contractors:**

Teresa Moroz-Kunicka, Mateusz Kunicki

***Project Coordinator***

## 1 Introduction

The electromagnetic field is described by two physical quantities: the electric field and the magnetic field. The electric field (also known as the electric component) is the component of the electromagnetic field expressed in  $V \cdot m^{-1}$ , and its value depends on the voltage. The magnetic field (also known as the magnetic component) is a component of the electromagnetic field expressed in  $A \cdot m^{-1}$ , and its value depends on the intensity of the flowing power. An additional feature that characterises the electromagnetic field in the case of alternating current is frequency. The frequency of the electricity grid is the same in the entire Polish and European power system and amounts to 50 Hz.

Protection of human health against the effects of the electromagnetic field (EMF) is carried out by setting limits (permissible values) for both components of the electromagnetic field in the environment. The legal act introducing such limits is the Regulation of the Minister of Health of 17 December 2019 *on permissible levels of electromagnetic fields in the environment* (Journal of Laws 2019, item 2448).

The regulation specifies different permissible levels of the electric field in the environment for places accessible to the public and areas intended for housing development. The regulation indicates:

- 1) the frequency ranges of electromagnetic fields for which the physical parameters characterising the electromagnetic field are determined;
- 2) the permissible values of the physical parameters referred to in item 1 for the individual frequency ranges to which the levels of electromagnetic fields refer.

For the electromagnetic field with a frequency of 50 Hz the above-mentioned regulation sets out the following limit values:

- 1) areas for places accessible to people:
  - a) electric component –  $10 \text{ kV} \cdot \text{m}^{-1}$ ,
  - b) magnetic component –  $60 \text{ A} \cdot \text{m}^{-1}$ ;
- 2) areas intended for housing development:
  - a) electric component –  $1 \text{ kV} \cdot \text{m}^{-1}$ ,
  - b) magnetic component –  $60 \text{ A} \cdot \text{m}^{-1}$ .

Therefore, it is assumed that the fields with the above-mentioned levels do not have a negative impact on any of the environmental elements (plants, animals), including humans, and do not show any cumulative effect.

The methods of measuring the electromagnetic field are specified in the Regulation of the Minister of Climate of 17 February 2020 *on the methods of checking compliance with the permissible levels of electromagnetic fields in the environment* (Journal of Laws of 2020, item 258).

Modelling of the distribution of the electric and magnetic components of the electromagnetic field was performed in the vicinity of the cable berm and the vicinity of busbars.

The terminology used in the study is consistent with the Technological Description of the Project provided by the Investor.

The results of the analyses presented in the study refer only to the object constituting the subject of the assessment.

## 2 Justification to exclude LPS from the calculations of electromagnetic field distribution

Computational determination of the distribution of the electric component of the electromagnetic field in the area of the designed station, which is characterised by a complex geometrical configuration of the current paths and structural elements, is a complicated issue. For the purposes of reports on the environmental impact of a project, no such calculations are made for the station area, assuming that the fenced station area, as an electric traffic area, is not accessible to unauthorised persons. Relatively good estimates of the electromagnetic field distribution are obtained by comparing the measurement results from other similar existing objects.

The results of measurements of the electric component of the electromagnetic field carried out for many domestic power stations with an upper voltage of 400, 220 and 110 kV indicate that in their vicinity there are no electric fields with the intensity exceeding  $1 \text{ kV}\cdot\text{m}^{-1}$  [limit value for areas intended for housing development (Regulation of the Minister of Health, Journal of Laws 2019, item 2448)]. The exceptions are usually places located in the vicinity of high-voltage overhead power lines entering the station area, where fields with an intensity not exceeding several  $\text{kV}\cdot\text{m}^{-1}$  are often found in the zone to the first support structure. It should be noted, however, that the source of these fields are not the station structures, but the overhead lines entering the area of the station (Szuba et al., 2008).

The main source of the magnetic field in the areas adjacent to the power station are also high-voltage overhead power lines entering its area. Much lower levels of the field are recorded in areas (outside the fenced station area) with no linear inputs and where the source of the magnetic field are the power buses of the station (connections in switch rooms) and the station apparatus (circuit breakers, instrument transformers, etc.).

In the vicinity of national high-voltage power stations, the highest values of the magnetic field are found in the vicinity of overhead lines entering the station area, which is justified by a shorter distance from the meter probe of the line conductors than the distance from the current paths (power buses) of the station. It should be noted that the intensity of the magnetic fields there are usually much lower than  $30 \text{ A}\cdot\text{m}^{-1}$ . Therefore they are below the limit value ( $60 \text{ A}\cdot\text{m}^{-1}$ ) established in the regulation (Regulation of the Minister of Health, Journal of Laws 2019 item 2448) for places accessible to people. In other places (apart from the station fence) the values of the magnetic field intensity are very small: from immeasurable to over a dozen  $\text{A}\cdot\text{m}^{-1}$ .

The conclusions presented above confirm the results of measurements of the electric and magnetic field intensity with a frequency of 50 Hz in the vicinity of the existing 220/110 kV Bydgoszcz Zachód power station, carried out by employees of the accredited Laboratory for Measurements of Electromagnetic Fields of the Wrocław University of Technology (Environmental Impact Assessment Report ...). Control measurements of the electric and magnetic field intensity were carried out near the existing power station, i.e. in the area between the fence of the station and the first pole of the line located outside the site. The results of the conducted measurements showed that at none of the measurement points the electric field intensity exceeded the permissible value of  $10 \text{ kV}\cdot\text{m}^{-1}$ . A slight exceedance of  $1 \text{ kV}\cdot\text{m}^{-1}$  occurred only near the line terminals. Moreover, the maximum value of the magnetic field intensity determined by the measurements occurred only in the vicinity of the line terminals and was much lower than the value allowed by the regulations.

Outside the fence of the station, the presence of electric fields with levels exceeding the permissible value in places accessible to people is not possible, mainly due to the considerable distance of live components from the fence of the station. Ensuring sufficiently large distances derives from the necessity to maintain sufficient electrical insulation gaps between the power bus and high voltage apparatus and all metal and grounded structures, e.g. the fence of the station. Such activities are

primarily aimed at ensuring failure-free operation of the facility, as well as the safety of people staying at the station. Thus, the significant distance between the live elements and the places where people are present means that there can be no question of the over-normative values of the electric and magnetic fields there.

To sum up, the results of measurements of the magnetic field intensity, which were conducted in the vicinity of a dozen or so high-voltage power stations in the country, lead to the conclusion that the magnetic fields generated by transmission lines entering the station are so small that in the light of today's knowledge on bio-electromagnetics, even in connection with the electric fields present there, they will not exert a negative impact on the flora and fauna, including the human body (Szuba et al., 2008).

Of course, in the area of the LPSs, there will be devices constituting sources of the electromagnetic field with different values of individual components. However, the LPSs will work without the permanent presence of workers within their premises, hence the exposure of workers to electromagnetic fields will occur only in the case of monitoring the operating conditions of devices in the stations and their maintenance, repairs and switching. the OSH rules in force at the stations will also ensure that the employees' exposure to electromagnetic fields is limited.

### 3 Theoretical foundations of computational methods

In the case of the designed busbars connecting the LPSs with the planned Choczewo PS and the cable lines used to transmit electricity from the Baltica OWF to the mentioned LPSs, the distribution of the electric and magnetic field intensity<sup>1</sup>, including the maximum value of each component of the field, was determined using computational methods.

Many computer programs calculate separately the distribution of each component of the electromagnetic field: electric (E) and magnetic (H). They most often use the so-called mirror superposition method, although there are also known computational algorithms based on the so-called finite element method.

According to the superposition principle, the electric (or magnetic) field at any point in the space surrounding the busbars or underground cable lines is the sum of the fields from all conductors of each of the busbars or cables that make up the cable berm.

In the case of busbars, to determine the electric field generated by charged bodies present in a heterogeneous environment (e.g. near the ground) the mirror reflection method is used. In this method, a heterogeneous environment with varied electric permittivity, in which charged bodies are placed, can be replaced with a homogeneous environment by introducing appropriate fictitious charges. When introducing fictitious charges, the condition of equality of the tangent components of the electric field intensity vector and the normal components of the electric induction vector at the boundary of the two environments must be met.

Most computer programs based on the mirror superposition method also use a simplifying assumption, according to which each wire of a line or busbar stretched between the support structures or gates (of the busbar), or each cable line is modelled with a rectilinear, infinitely long wire, with a diameter characteristic for a specific type of real conductor or cable.

The computational algorithms for the analysis of the distribution of the electric (E) and magnetic (H) fields generated by overhead power lines are complex and can also be used to analytically determine the distribution of individual components accompanying the operation of busbars. It should be emphasised that for the calculations of the E or H distribution, which are most often carried out in a cross section perpendicular to the axis of the line or the busbar, as well as the cable berm<sup>2</sup> (only the magnetic component), the designed smallest distances between the conductors (power buses) or cables and the calculation point are always assumed because, in these places, the maximum values of the individual components of the field should be expected. This means that in the case of busbars, calculations of the electric and magnetic field distribution (including the maximum values of individual components) are performed for the shortest distance of the phase conductors from the ground. In the case of cable lines, calculations of the magnetic field distribution above the line are performed for the smallest<sup>3</sup> projected depth of the cable lines immersion, because in such conditions the maximum values of this component should be expected.

---

<sup>1</sup>In the case of cable lines, it is challenging to speak of determinations of the electric field intensity distribution outside the cable sheath. This field, identified outside the cable's outer sheath, is negligibly small due to the screening properties of the cable shields.

<sup>2</sup>In complex power supply systems, cable lines placed in the ground (in the soil) in the so-called cable channels are formed by (supplying) cable routes, called a cable berm in the TDP provided by the Investor.

<sup>3</sup>It should be remembered that along the entire length of the cable line, the depth at which the cables are buried in the ground may be different, and the calculations of the magnetic field intensity distribution are performed for the smallest of these depths.



## 4 Distribution of the electromagnetic field intensity in the vicinity of the designed cable berm

### 4.1 Technical parameters of the designed cable berm

The design documentation stipulates that power from the Baltica OWF will be sent to the LPSs via cable lines operating at a voltage of 220 or 275 kV.

Each of the cable lines, which will consist of 3 single-phase cables with copper or aluminium conductors (phases: L1, L2, and L3), will be laid in a trench (or tunnel), an exemplary cross-section of which is presented in the figure below [Figure 4.1]. The distance between the axes of individual cables in each cable line will be approx. 0.3 m.

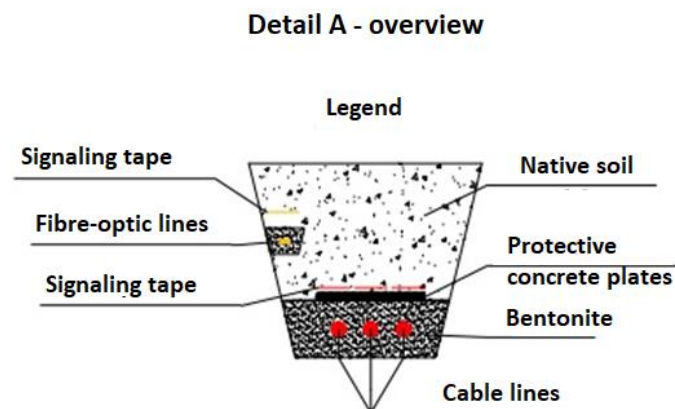


Figure 4.1. An example of a cross-section of an open trench with 3 single-phase cables with copper or aluminium conductors, constituting a single cable line

Source: internal data

The cable lines will be laid flat in the native soil at a depth of 1.5 m (the upper cable sheath). The designed mutual distance between the axes of cable lines is 5.0 m.

Individual cable lines (9 in the case of the Applicant's variant – APV – or 11 in the case of the rational alternative variant – RAV) will be carried out parallel to form the cable berm [Figure 4.2].

Environmental Impact Assessment Report on the Connection Infrastructure of the Baltica-2 and Baltica-3 Offshore Wind Farms Appendix 3 – Electromagnetic field modelling (...)

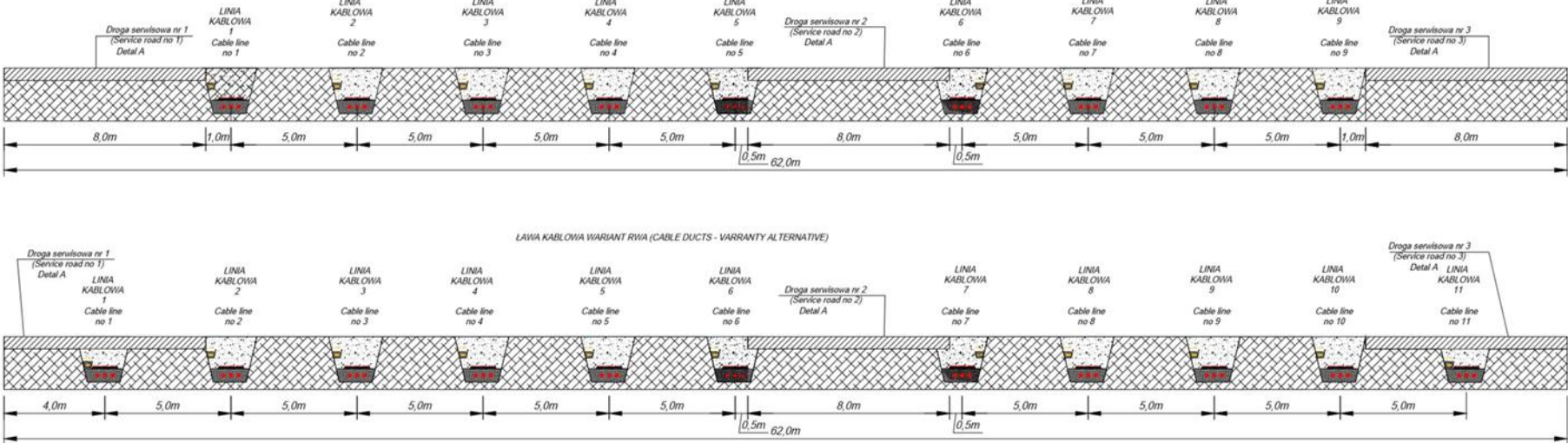


Figure 4.2. The cross-section of the Baltica OWF CI cable berm (top – APV – 9 cable lines, bottom – RAV – 11 cable lines)

Source: internal data

Table 4.1. Technical data of the cable berm introducing power from the Baltica OWF into LPSs adopted for the modelling of the EMF distribution

No.	Technical data	Value or description
1	The distance between the symmetry axes of the cable lines	5 m
2	Arrangement of cables in individual cable lines	Flat
3	the distance between the axes of individual cables in each cable line	0.3 m
4	Cable diameter	135 mm
5	Cable insertion depth (distance from the earth surface to the cable sheath)	1.5 m
6	Phase layout in each cable line	Starting from the south: L1 L2 L3 ...L1 L2 L3... L1 L2 L3.....
7	Distance between cable trays B2 and B3 (according to Figure 4.3 for the APV and RAV)	9 m for both variants

Source: internal data

## 4.2 Assumptions for the calculation of the magnetic field distribution in the vicinity of the designed cable berm

In the case of cable lines, only the magnetic component of the electromagnetic field will be introduced into the environment (the electrical component is shielded by the conductive core of the cable sheath, mainly a steel braiding).

All calculations of the magnetic field intensity distribution were made with the use of the PoE-M<sup>4</sup> computer program, the algorithm of which is based on the following assumptions:

- 1) APV (the contractor's variant): 9 cable lines, each of which consists of 3 single cables supplied with an alternating voltage of 220 or 275 kV, with a permissible current carrying capacity  $I_{max}$ :
  - Solution 1:
    - Baltica-2 – voltage of 275 kV – 914 A,
    - Baltica-3 – voltage of 275 kV – 819 A;
  - Solution 2:
    - Baltica-2 – voltage of 220 kV – 1140 A,
    - Baltica-3 – voltage of 220 kV – 1024 A;
- 2) RAV (rational alternative variant): 11 cable lines, each of which consists of 3 single cables supplied with an alternating voltage of 220 or 275 kV, with the permissible current carrying capacity of each cable  $I_{max}$ :
  - Solution 1:
    - Baltica-2 – voltage of 275 kV – 730 A,
    - Baltica-3 – voltage of 275 kV – 614 A;
  - Solution 2:
    - Baltica-2 – voltage of 220 kV – 912 A,
    - Baltica-3 – voltage of 220 kV – 768 A.

Technical data of the cable berm comply with the table above [Table 4.1].

The location of the computation cross-section, in which the distribution of the magnetic field intensity was determined, is presented in the figure below [Figure 4.3].

<sup>4</sup>Author's proprietary program. Author: D.Sc., Eng. Marek Szuba, Consulting and Engineering Office „EKO-MARK”.

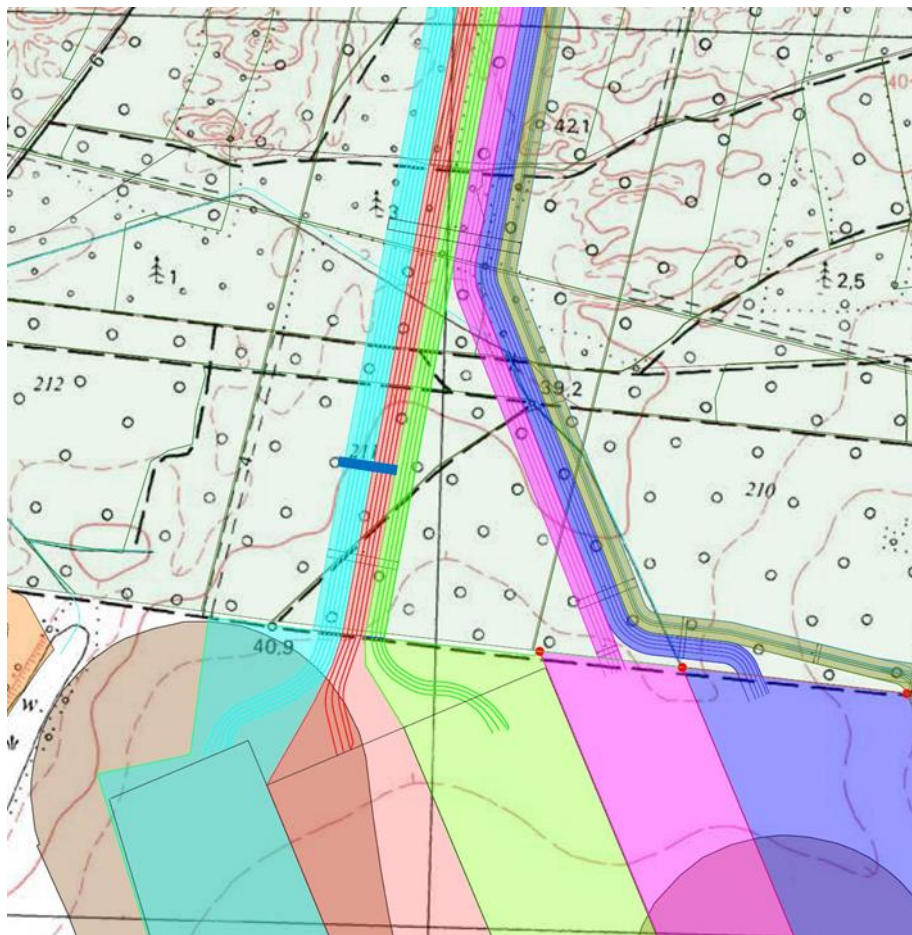


Figure 4.3. Location of the computation cross-section in which the distribution of the magnetic field intensity was determined

Source: internal data

The place of the vertical axis on the graphs illustrating the magnetic field distributions is in the middle of the distance between the extreme cables of all the analysed cable lines.

Calculations of the magnetic field distribution for individual variants (APV and RAV) were conducted by identifying the values of the said quantity at the levels of 0.2; 1.0 and 2.0 m a.g.l. following the recommendation indicated in the regulation (Regulation of the Minister of Climate, Journal of Laws 2020, item 258).

### 4.3 The results of calculations of the magnetic field distribution in the vicinity of the designed cable berm

The calculation results of the maximum values of the magnetic field intensity (H) that can be expected above the cable line for the APV are presented in the table below [Table 4.2], while the results for the RAV are presented in the next table [Table 4.3]. Graphs of the magnetic field intensity (H) cross-section to the axis of the cable berm are shown in the following figures [Figure 4.4–Figure 4.15].

Table 4.2. Calculation results of the expected maximum magnetic field intensities in the vicinity of the cable berm for the APV (9 cable lines, flat layout)

Solution	Voltage [kV]	B2	B3	The maximum expected value of the magnetic field intensity H [ $A \cdot m^{-1}$ ] determined at individual levels [m a.g.l.]

						0.2	1.0	2.0
		Number of cable lines	$I_{max}$ [A]	Number of cable lines	$I_{max}$ [A]			
1	275	5	914	4	819	22.1	10.2	5.8
2	220		1140		1024	27.6	12.7	7.2

Source: internal data

Table 4.3. Calculation results of the expected maximum magnetic field intensities in the vicinity of the cable berm for the RAV (11 cable lines, flat layout)

Solution	Voltage [kV]	B2		B3		The maximum expected value of the magnetic field intensity H [ $A \cdot m^{-1}$ ] determined at individual levels [m a.g.l.]		
		Number of cable lines	$I_{max}$ [A]	Number of cable lines	$I_{max}$ [A]	0.2	1.0	2.0
2	220	912	768	21.8	10.2	5.7		

Source: internal data

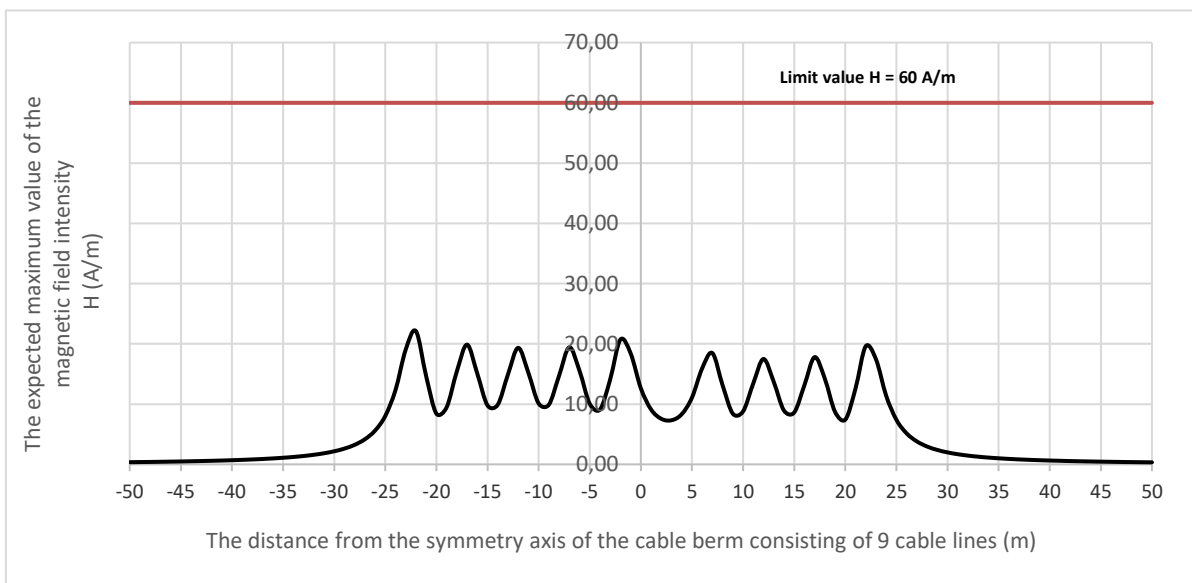


Figure 4.4. The expected maximum magnetic field intensity (H) at a level of 0.2 m a.g.l. as a function of the distance from the axis of the cable berm (APV, Solution 1)

Source: internal data

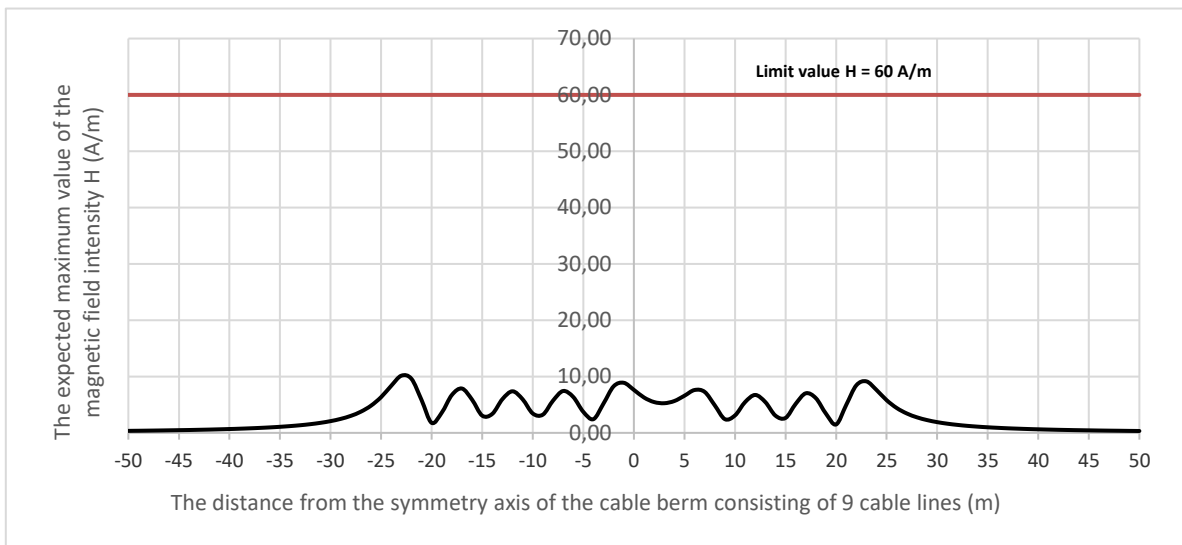


Figure 4.5. The expected maximum magnetic field intensity ( $H$ ) at a level of 1.0 m a.g.l. as a function of the distance from the axis of the cable berm (APV, Solution 1)

Source: internal data

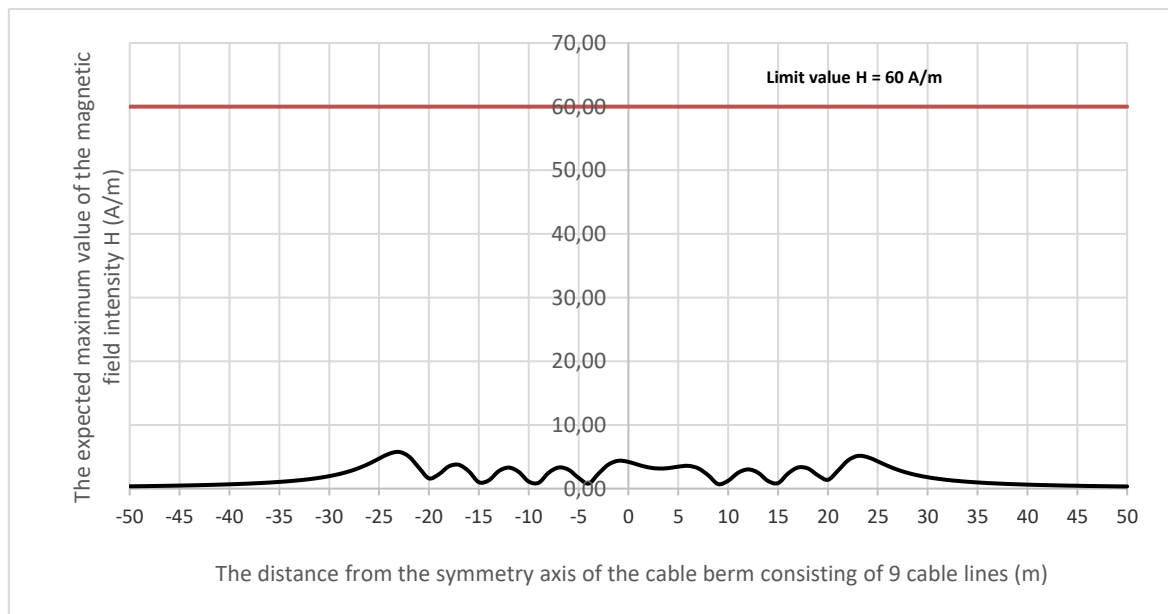


Figure 4.6. The expected maximum magnetic field intensity ( $H$ ) at a level of 2.0 m a.g.l. as a function of the distance from the axis of the cable berm (APV, Solution 1)

Source: internal data

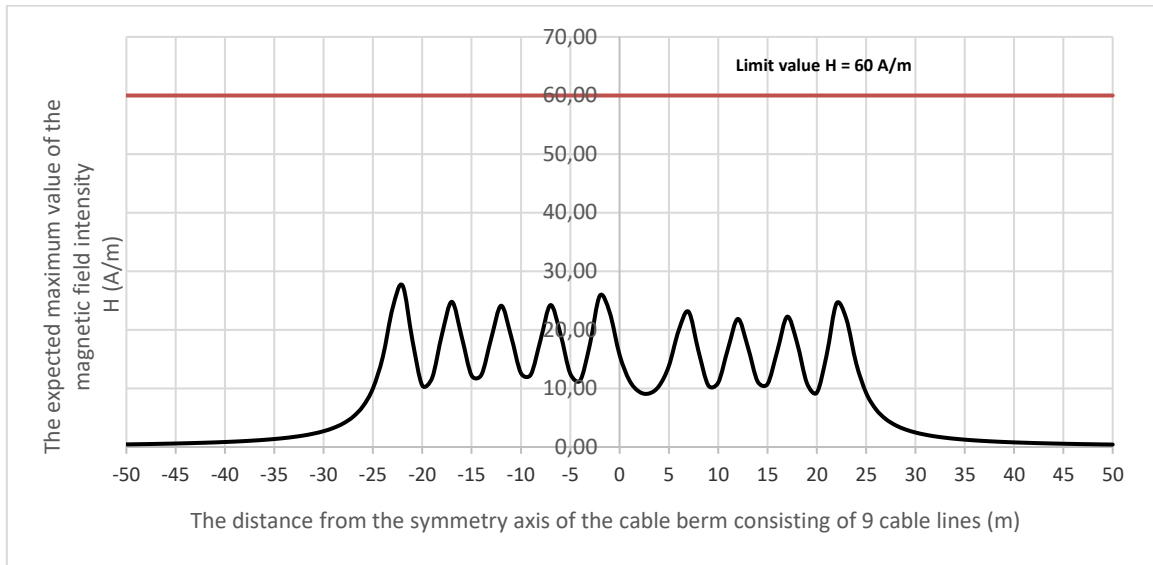


Figure 4.7. The expected maximum magnetic field intensity (H) at a level of 0.2 m a.g.l. as a function of the distance from the axis of the cable berm (APV, Solution 2)

Source: internal data

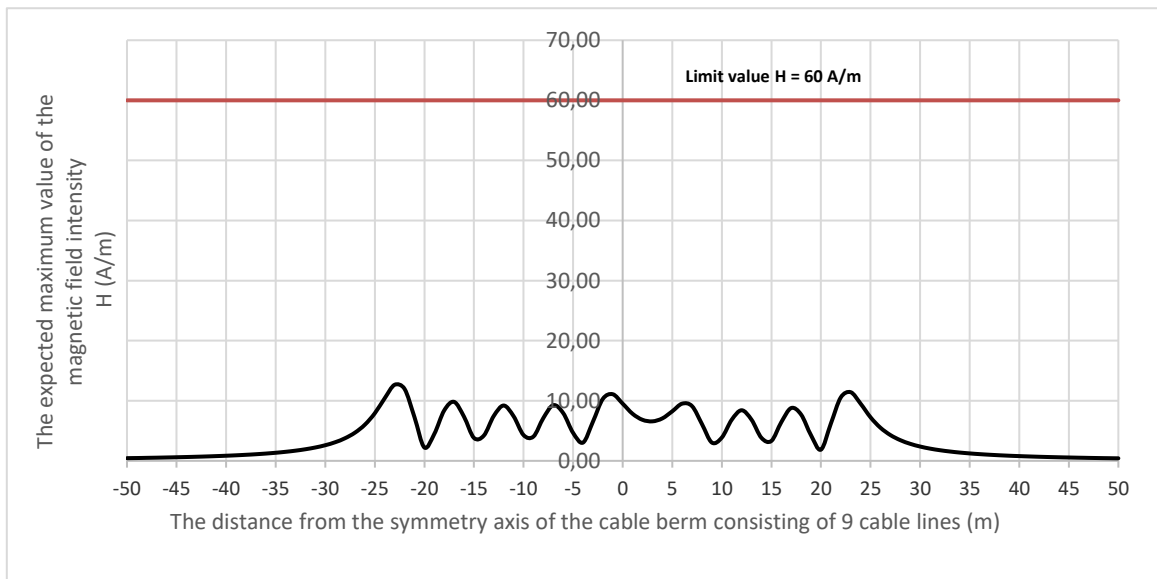


Figure 4.8. The expected maximum magnetic field intensity (H) at a level of 1.0 m a.g.l. as a function of the distance from the axis of the cable berm (APV, Solution 2)

Source: internal data

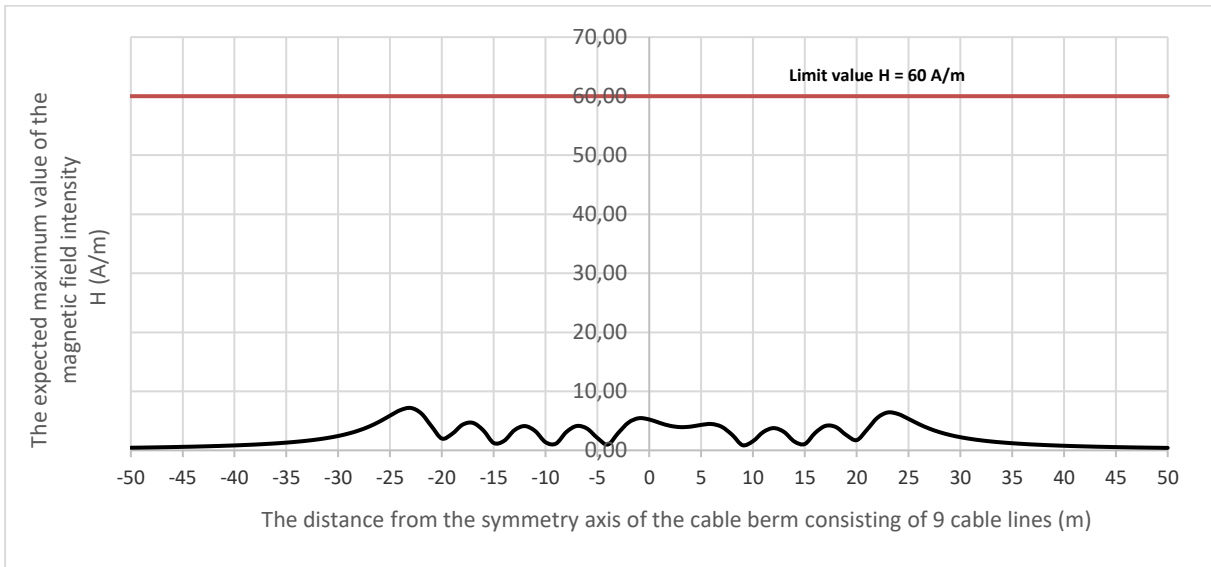


Figure 4.9. The expected maximum magnetic field intensity ( $H$ ) at a level of 2.0 m a.g.l. as a function of the distance from the axis of the cable berm (APV, Solution 2)

Source: internal data

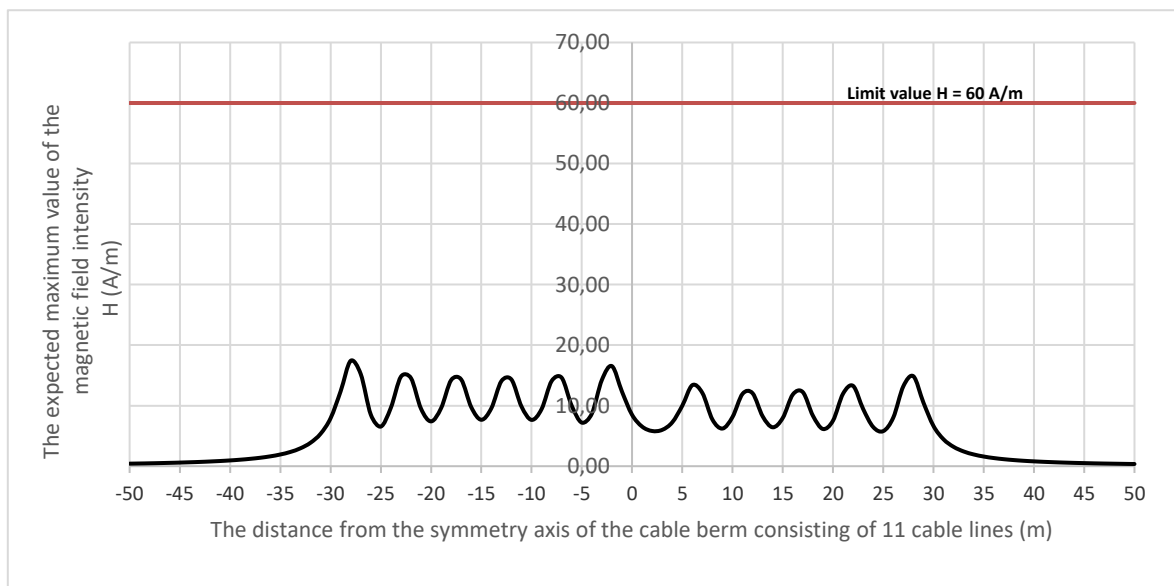


Figure 4.10. The expected maximum magnetic field intensity ( $H$ ) at a level of 0.2 m a.g.l. as a function of the distance from the axis of the cable berm (RAV, Solution 1)

Source: internal data



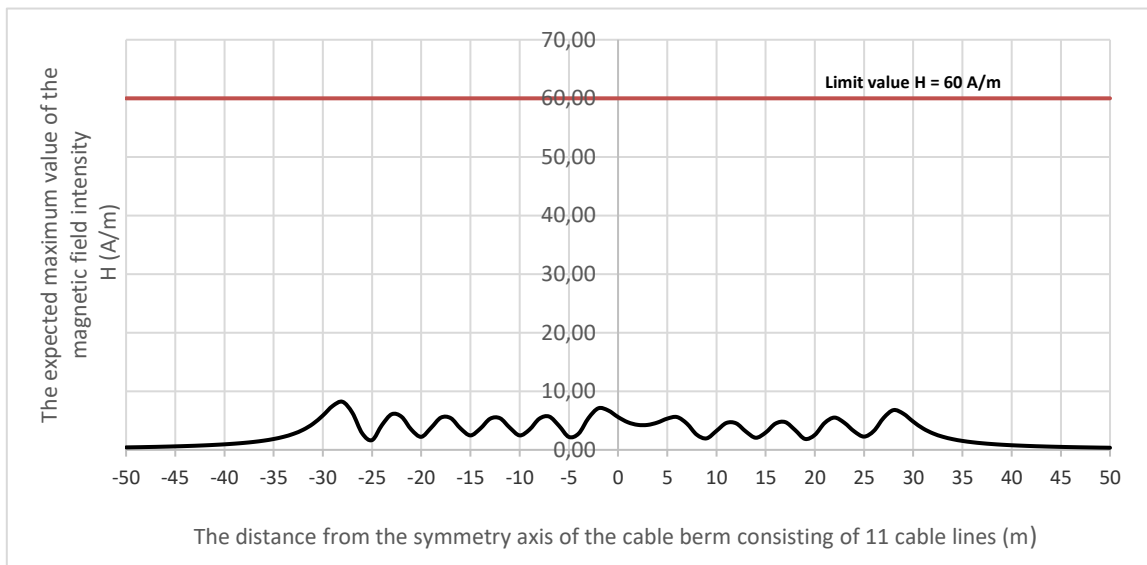


Figure 4.11. The expected maximum magnetic field intensity ( $H$ ) at a level of 1.0 m a.g.l. as a function of the distance from the axis of the cable berm (RAV, Solution 1)

Source: internal data

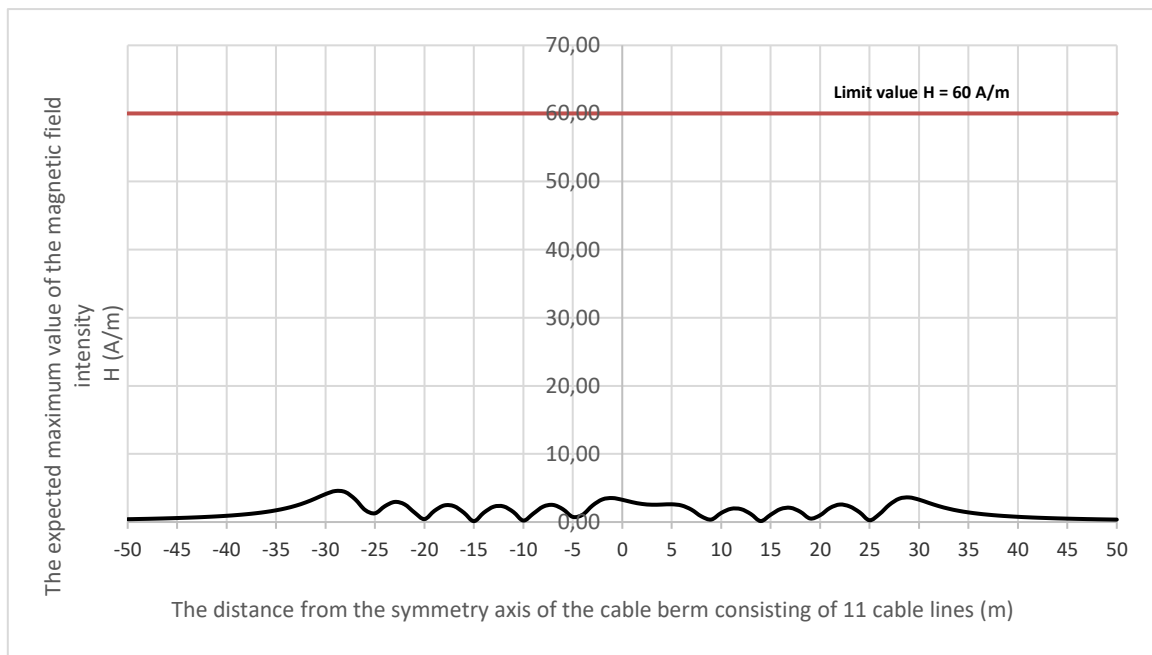


Figure 4.12. The expected maximum magnetic field intensity ( $H$ ) at a level of 2.0 m a.g.l. as a function of the distance from the axis of the cable berm (RAV, Solution 1)

Source: internal data

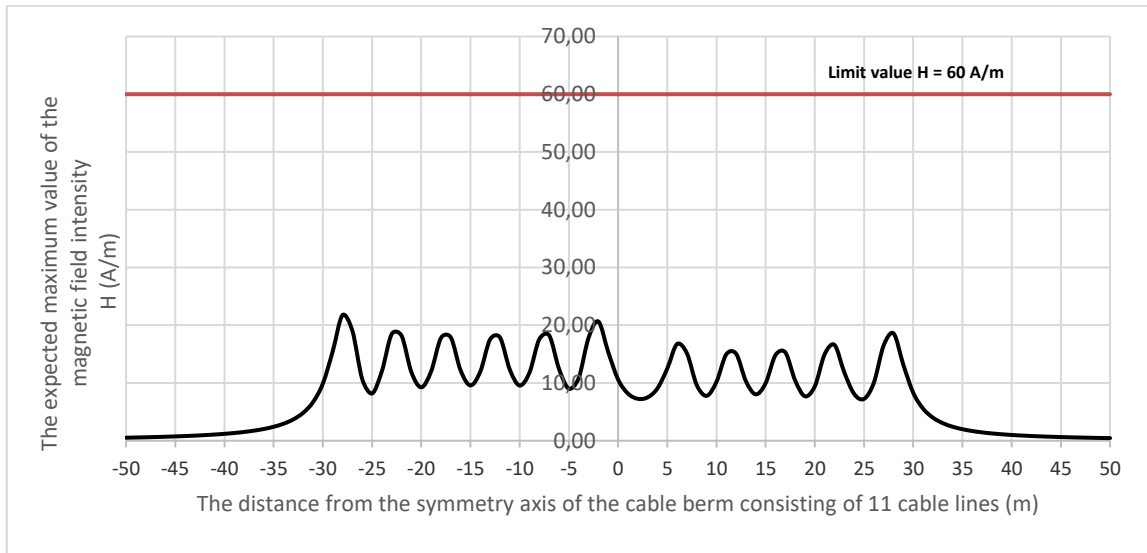


Figure 4.13. The expected maximum magnetic field intensity (H) at a level of 0.2 m a.g.l. as a function of the distance from the axis of the cable berm (RAV, Solution 2)

Source: internal data

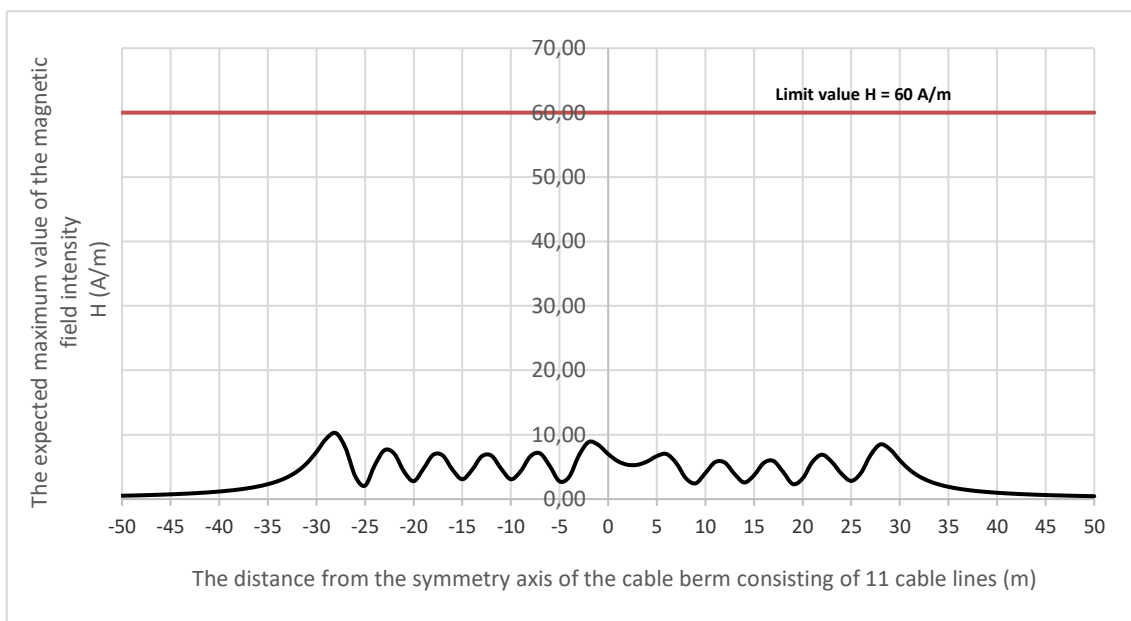


Figure 4.14. The expected maximum magnetic field intensity (H) at a level of 1.0 m a.g.l. as a function of the distance from the axis of the cable berm (RAV, Solution 2)

Source: internal data

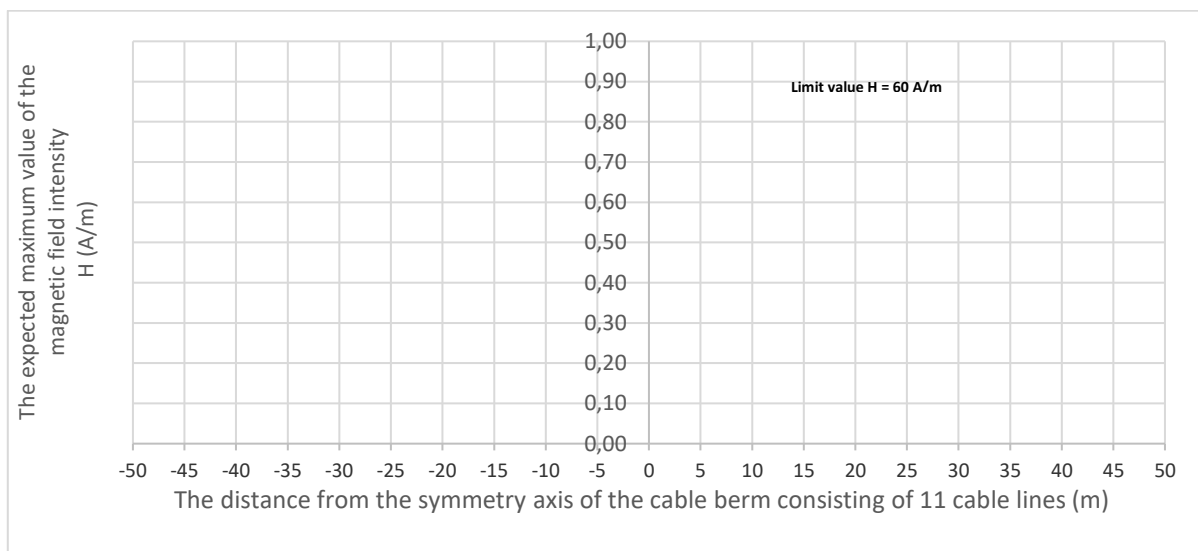


Figure 4.15. The expected maximum magnetic field intensity (H) at a level of 2.0 m a.g.l. as a function of the distance from the axis of the cable berm (RAV, Solution 2)

Source: internal data

#### 4.4 Interpretation of the computation results

Computations of the distribution of the magnetic field (H) generated by the cable berm that powers the LPSs, conducted for two design variants, i.e. APV (9 cable lines) and RAV (11 cable lines), showed that in none of the variants (assuming the maximum current carrying capacity of each cable line), will the permissible value of this field intensity exceed the limit value ( $H_{perm} = 60 \text{ A}\cdot\text{m}^{-1}$ ) established in the regulations (Regulation of the Minister of Health, Journal of Laws 2019, item 2448) for places accessible to people in the height range from 0.2 m to 2.0 m a.g.l.

## 5 The distribution of the electromagnetic field intensity in the vicinity of busbars

### 5.1 Assumptions for the computation of the electric and magnetic field intensity distribution in the vicinity of busbars

The analysis of theoretical relationships that determine the computation algorithm shows that the maximum value and the distribution of the electric (E) and magnetic (H) field intensity in the vicinity of busbars are influenced mainly by the following parameters:

- phase voltage of the busbars (affects only the distribution of the electric field intensity);
- the load current of each busbar (affects only the distribution of the magnetic field intensity);
- the distance between the ground and the busbar (in the analysed case, the cable bridge);
- the spacing between the conductors forming the busbar;
- the phase conductor system (phase configuration) in adjacent busbars.

Other constructional elements of the busbar have a smaller impact on the distribution of the electric and magnetic field intensity. In addition, the distribution of the electric field intensity in the vicinity of busbars is influenced by conductive elements in the environment located in their immediate vicinity, such as metal structures (e.g. fencing), buildings, etc. Determining the impact of these elements on the distribution of the electric field in the vicinity of busbars is generally possible only if it is based on measurements.

The distributions of both the electric and magnetic fields change depending on the phase arrangement in individual conductors (cords) forming the busbars. Thus, to calculate the distributions of both field components, the phase arrangement in the individual conductors (lines) of the busbar proposed in the technical documentation was adopted.

With a specific structure of the conductors (cords) forming the busbar and the assumed phase configuration, as well as with a determined value of the phase voltage<sup>5</sup>, the electric field intensity in the vicinity of each busbar depends primarily on the distance between the conductors (cords) and the ground. The field intensity increases with a decrease in this distance, and the greatest value is obtained in the cross-section<sup>6</sup> in which the distance between the conductors (cords) from the ground is the smallest.

For the model calculations of the distribution of the electric (E) and magnetic (H) field intensity, the following parameters of each of the 4 busbars declared in the project were adopted:

- voltage rating of the busbar [kV]  $U_n = 400$  kV (calculations were made for the least favourable scenario, i.e. maximum operating voltage:  $U_{max} = 420$  kV);
- estimated load current of the busbar:  $I_{max} = 2300$  A;
- power buses: each phase of the busbar is made in the form of a three-wire beam of steel-aluminium cables with an estimated diameter of 26 mm; cables configured in an equilateral triangle with the apex downwards and with a side length of 40 cm; solutions are allowed in the connections of busbars including a quadrangular four-wire beam system;
- the shortest distance from the ground of the conductors forming each of the busbars  $h_{min} = 13.0$  m;

---

<sup>5</sup>For example, the phase voltage with a voltage rating of 400 kV can vary from 380 kV to 420 kV.

<sup>6</sup>(Calculation) cross-section is a section of a straight line, usually perpendicular to the busbar, along which, in the assumed distance range, the electric and magnetic field strength is calculated, usually at points separated by 1 m.

- the distance between the axes of the phase conductors (axes of the three-conductor beams) in each busbar: at least 6.0 m;
- 2 lightning conductors are installed above each busbar gate<sup>7</sup>;
- phase arrangement in busbars:
  - configuration A: L1, L2, L3;      L1, L2, L3;      L1, L2, L3;      L1, L2, L3,
  - configuration B: L1, L2, L3;      L3, L2, L1;      L1, L2, L3;      L3, L2, L1.

Calculations of the electric field distribution (similarly to the magnetic field) were carried out in the cross-section presented in the figure below [Figure 5.1] (on the road between the LPS fence and the fence of the Choczewo PS). In this cross-section, the distance from the ground of the conductors forming each of the busbars is the smallest along the length of the entire busbar system and it is:  $h = h_{\min} = 13.0$  m. As a consequence, the electric (and magnetic) field intensity can reach maximum values there, while the intensity of both the field components in any other place under all busbars will certainly be smaller than those determined in the indicated cross-section; in the area of the LPSs, slightly higher values can be expected.



Figure 5.1. The location of the busbars evacuating power from the LPSs and the location of the computational cross-section along which the distribution of the electric and magnetic field was determined

Source: internal data

At this point it should be stated that the purpose of the calculations is to check whether, under the technical assumptions adopted in the design documentation, environmental quality standards may be exceeded, also under the most unfavourable operating conditions for the busbars (the smallest designed distance between the conductors/power buses from the ground and the maximum phase voltage and current carrying capacity of the busbars) that evacuate electric power out of the LPSs. As already mentioned, the maximum intensity of the electric field  $E_{\max}$  and magnetic field  $H_{\max}$  under the conductors of the busbars (in places accessible to people) should be expected in the place where the distance between the ground and the conductors of each busbar is the smallest ( $h = h_{\min}$ ). Therefore, the calculations were carried out for the smallest designed distance between the phase conductor (the cables forming the rail bridge) and the ground,  $h_{\min} = 13.0$  m. The results of calculations of the electric (E) and magnetic (H) field intensity distributions, which were conducted for the above-described cross-section [Figure 5.1] and two different phase configurations are presented in the following figures [Figure 5.2–Figure 5.5].

<sup>7</sup> Lightning protection cables are not a source of either an electric or magnetic field. It is possible that an optical fibre cable is also installed in the lightning conductor.

## 5.2 The results of calculations of the electric and magnetic field distribution in the vicinity of busbars

The results of the calculations of the expected maximum intensities of the electric (E) and magnetic (H) field determined at a level of 2.0 m a.g.l., assuming the least favourable operating conditions for busbars from the environmental point of view, i.e.  $U_n = 400$  kV ( $U_{max} = 420$  kV) with the permissible current carrying capacity of each busbar  $I_{max} = 2300$  A, are summarised in the table below [Table 5.1], while the distributions of the electrical (E) and magnetic (H) components of the electromagnetic field in the calculation cross-section presented below [Figure 5.1] are shown in the following figures for two-phase configurations [Figure 5.2–Figure 5.5]. The computations were conducted for the operating voltage ( $U_{max} = 420$  kV).

Table 5.1. Computation results of the expected maximum intensities of electric (E) and magnetic (H) field in the vicinity of 4 busbars in two-phase configurations (configuration A and B)

The maximum working voltage of the busbar (permissible in the long term) $U_{max} = 420$ kV; The maximum current carrying capacity of each busbar $I_{max} = 2300$ A			
The maximum expected intensity of the electric field E [ $kV \cdot m^{-1}$ ]		The maximum expected intensity of the magnetic field H [ $A \cdot m^{-1}$ ]	
Configuration A	Configuration B	Configuration A	Configuration B
3.9	4.2	22.5	26.4

Source: internal data

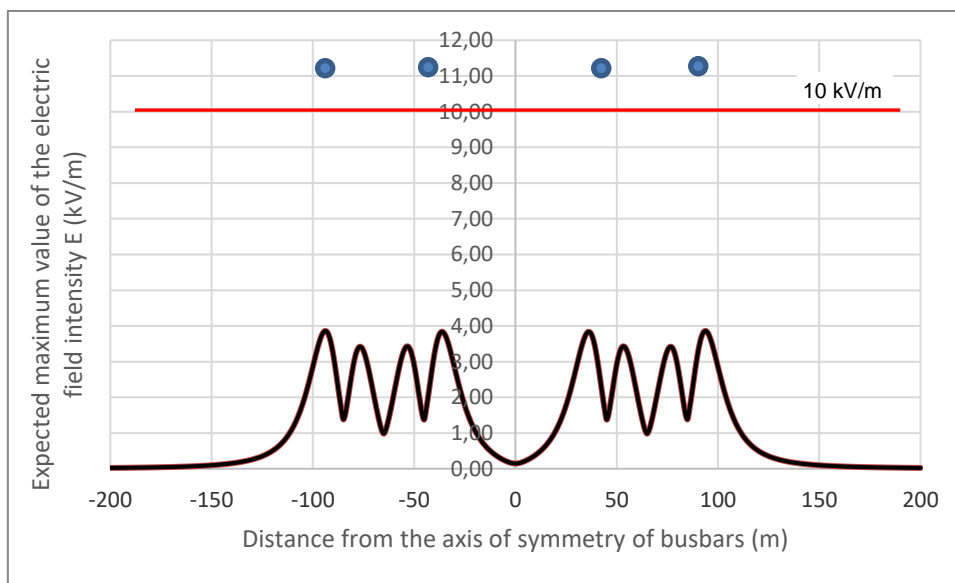


Figure 5.2. The expected maximum intensity of the electric field (E) at a level of 2.0 m a.g.l. as a function of the distance from the axes of 4 busbars (the axes of symmetry of individual busbars are characterised by the following coordinates: busbar 1: -85 m, busbar 2: -45 m, busbar 3: +45 m, busbar 4: +85 m). The figure below presents the positions of the middle phases (L2) of each busbar (dark blue dots). Phase configuration: A.  $10 kV \cdot m^{-1}$  – permissible electric field intensity for places accessible to people

Source: internal data

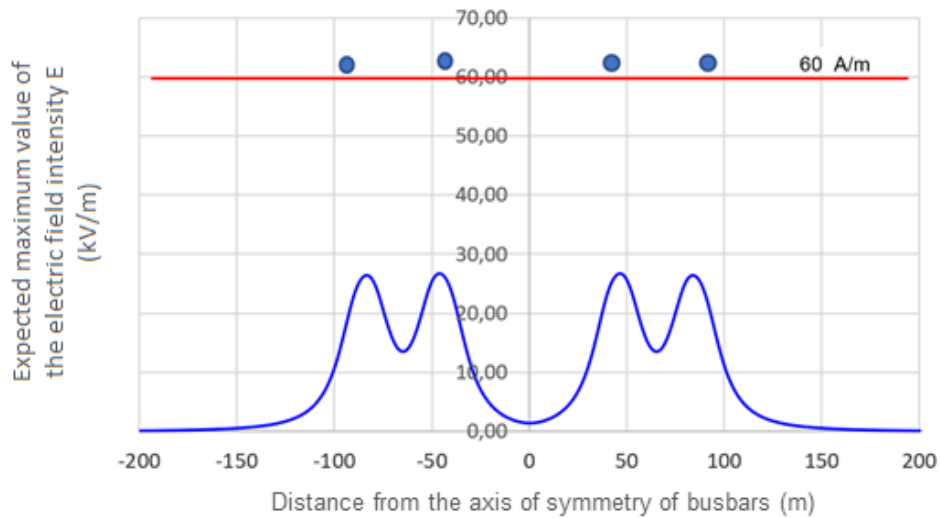


Figure 5.3. The expected maximum intensity of the magnetic field (H) at a level of 2.0 m a.g.l. as a function of the distance from the axes of 4 busbars (the axes of symmetry of individual busbars are characterised by the following coordinates: busbar 1: -85 m, busbar 2: -45 m, busbar 3: +45 m, busbar 4: +85 m). The figure below presents the positions of the middle phases (L2) of each busbar (dark blue dots). Phase configuration: A

Source: internal data

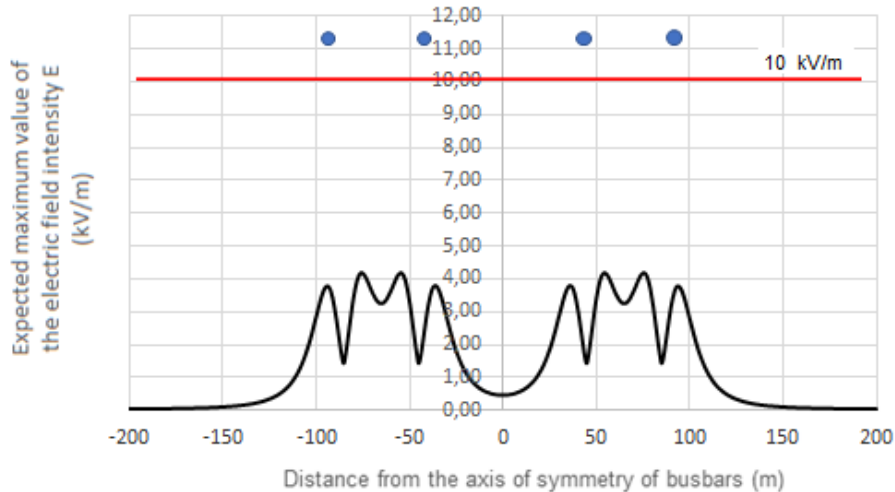


Figure 5.4. The expected maximum intensity of the electric field (E) at a level of 2.0 m a.g.l. as a function of the distance from the axes of 4 busbars (the axes of symmetry of individual busbars are characterised by the following coordinates: busbar 1: -85 m, busbar 2: -45 m, busbar 3: +45 m, busbar 4: +85 m). The figure below presents the positions of the middle phases (L2) of each busbar (dark blue dots). Phase configuration: B.  $10 \text{ kV}\cdot\text{m}^{-1}$  – permissible electric field intensity for places accessible to people

Source: internal data

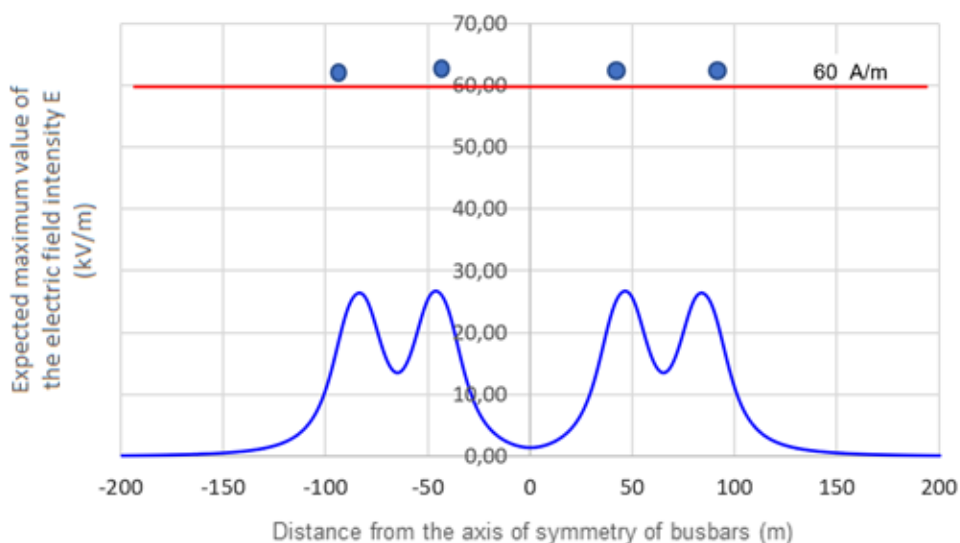


Figure 5.5. The expected maximum intensity of the magnetic field ( $H$ ) at a level of 2.0 m a.g.l. as a function of the distance from the axes of 4 busbars (the axes of symmetry of individual busbars are characterised by the following coordinates: busbar 1: -85 m, busbar 2: -45 m, busbar 3: +45 m, busbar 4: +85 m). The figure below presents the positions of the middle phases (L2) of each busbar (dark blue dots). Phase configuration: B

Source: internal data

### 5.3 Interpretation of the computation results

Computations of the electric ( $E$ ) and magnetic ( $H$ ) field distribution, which were carried out for the shortest distance between the ground and the phase conductors (cords) forming the busbars ( $h = h_{\min} = 13.0$  m), showed that the electric field intensity ( $E$ ) under the four busbars in total, identified at a level of 2.0 m a.g.l., will not exceed the value:  $3.9 \text{ kV}\cdot\text{m}^{-1}$  – for the bus configuration A and  $4.2 \text{ kV}\cdot\text{m}^{-1}$  – for the bus configuration B. Therefore, regardless of the configuration, the maximum electric field intensity will be significantly lower than the permissible value ( $10 \text{ kV}\cdot\text{m}^{-1}$ ) established in the regulation (Regulation of the Minister of Health, Journal of Laws 2019, item 2448) for places accessible to people.

The nearest existing housing development is at a distance of 520 m, and the planned housing development is at a distance of 385 m from the axis of the four busbars. Therefore, both the existing and planned housing developments are located in an area where the electric field intensity is much lower than  $1 \text{ kV}\cdot\text{m}^{-1}$  (the limit value for areas intended for housing development).

Calculations of the magnetic field distribution ( $H$ ) showed that its intensity under four busbars, identified at a level of 2.0 m a.g.l. under the least favourable operating conditions for busbars, will not exceed the value of  $22.5 \text{ A}\cdot\text{m}^{-1}$ , so it will be significantly lower than the permissible value ( $60 \text{ A}\cdot\text{m}^{-1}$ ) set out in the regulation (Regulation of the Minister of Climate, Journal of Laws 2020, item 258) for places accessible to people.



## 6 The distribution of the cumulative magnetic field intensity

### 6.1 Assumptions for the calculation of the cumulative magnetic field distribution in the vicinity of the designed cable berm

Investments of four other developers will be built in the vicinity of the Baltica OWF CI: Baltica 1, Baltex<sup>8</sup>, Baltic Power and Ocean Winds. Electricity generated in the offshore wind farms will be sent from each of them through cable lines operating at 220 or 275 kV. Almost along the entire length of the route, the cables supplying subscriber stations of the above-mentioned developers will be run in a common cable berm. From the point of view of environmental impact, it is interesting to analyse the cumulative level of the magnetic field from all simultaneously operating cable lines. In practice, this comes down to the determination of the magnetic field distribution generated by all cable lines run in parallel in a common cable berm. Taking into account the variant design solutions for the lines supplying the end-user stations of Baltica-2 and Baltica-3, referred to in subsection 4.1 (APV and RAV variants), and taking into account the technical data of cable lines obtained from the developers of the Baltex, Baltic Power and Ocean Winds, the cable berm, the location of which in the field is shown in the figure below [Figure 6.1], will consist of 23 (APW) or 25 (RAV) cable lines.

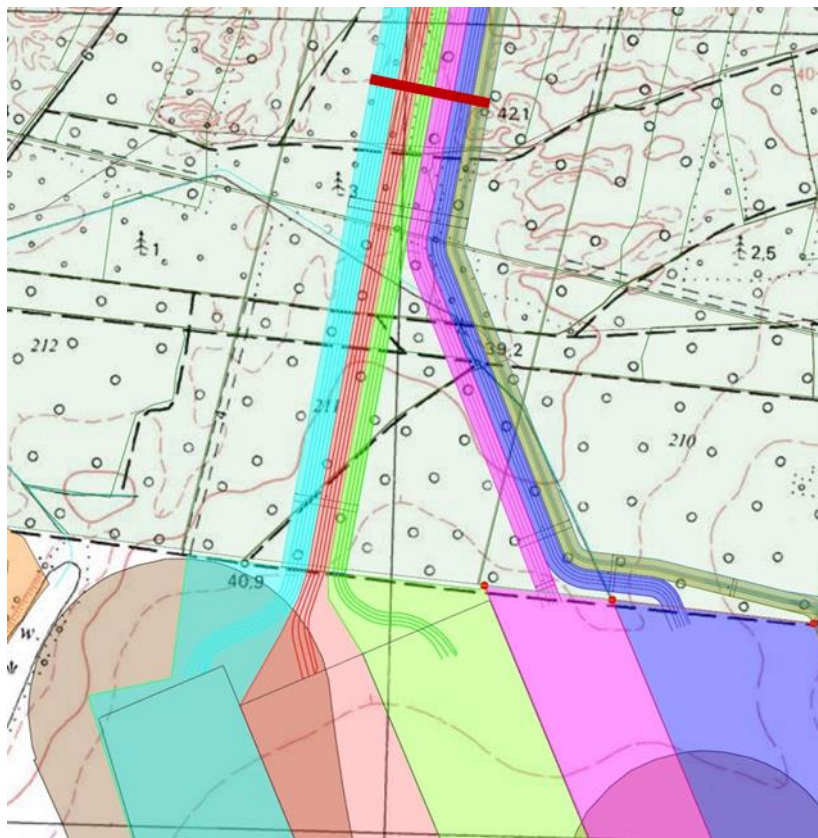


Figure 6.1. Location of the computational cross-section in which the distribution of the cumulative magnetic field intensity was determined

Source: internal data

<sup>8</sup> Baltex is a historic name. Currently, the procedure of assigning the PSzW to participating entities is underway. It is possible that another company will get the permit. This name has been used in this document to clearly distinguish the infrastructure. However, this should be treated as a reserve for the future entity that will acquire the PSzW permit and the technical conditions for connection to the PSE substation.

The number and electrical parameters of individual cable lines adopted for modelling the distribution of the cumulated magnetic field are summarised in the table below [Table 6.1]. As a consequence of the assumptions adopted, calculations of the cumulative magnetic field intensity distribution were carried out for four models taking into account both power supply variants of Baltica-2 and Baltica-3 end-user stations (APV and RAV), considered for two analysed levels of the rated voltage of the cable lines ( $U_n = 275 \text{ kV}$  – Solution 1 and  $U_n = 220 \text{ kV}$  – Solution 2).

As mentioned earlier, all cable lines will run parallel in a common cable berm. The configuration of individual cable lines in the cable tray is shown in the figures below – [Figure 6.2] (APV) and [Figure 6.3] (RAV), while the technical data adopted for the process of modelling the cumulative magnetic field distribution are presented in the table below [Table 6.2].

Table 6.1. Technical data of simultaneously operating power supply systems powering the end-user stations: Baltica 2, Baltica 3, Baltica 1, Baltex, Baltic Power, and Ocean Winds adopted for modelling the distribution of the cumulative magnetic field in the cross-section shown in the figure above [Figure 6.1]

Model	Variant (Baltica)	Solution	Baltica 2	Baltica 3	Baltica 1	Baltex	Baltic Power	Ocean Winds	Total number	
									power lines	cables
M1	APV	Solution 1	U = 275 kV I = 914 A	U = 275 kV I = 819 A	U = 275 kV I = 819 A	U = 275 kV I = 721 A	U = 275 kV I = 890 A	U = 275 kV I = 552 A	23	69
			5 lines	4 lines	4 lines	4 lines	4 lines	2 lines		
M2		Solution 2	U = 220 kV I = 1140 A	U = 220 kV I = 1024 A	U = 220 kV I = 1024 A	U = 220 kV I = 902 A	U = 220 kV I = 830 A	U = 220 kV I = 691 A		
			5 lines	4 lines	4 lines	4 lines	4 lines	2 lines		
M3	RAV	Solution 1	U = 275 kV I = 730 A	U = 275 kV I = 614 A	U = 275 kV I = 614 A	U = 275 kV I = 721 A	U = 275 kV I = 890 A	U = 275 kV I = 552 A	25	75
			6 lines	5 lines	4 lines	4 lines	4 lines	2 lines		
M4		Solution 2	U = 220 kV I = 912 A	U = 220 kV I = 768 A	U = 220 kV I = 768 A	U = 220 kV I = 902 A	U = 220 kV I = 830 A	U = 220 kV I = 691 A		
			6 lines	5 lines	4 lines	4 lines	4 lines	2 lines		

Source: internal data

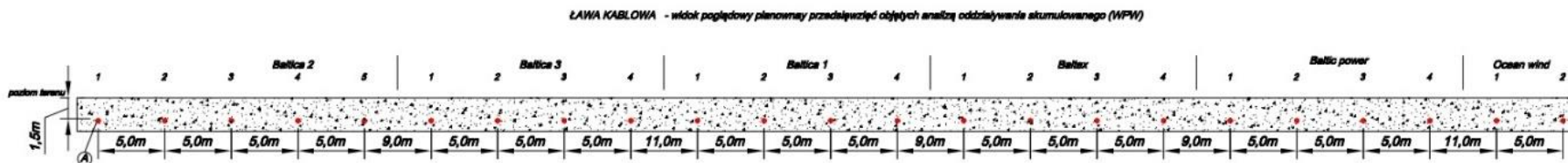


Figure 6.2. The arrangement of individual cable lines in the cable berm as adopted for the modelling of the cumulative magnetic field distribution – APV

Source: internal data

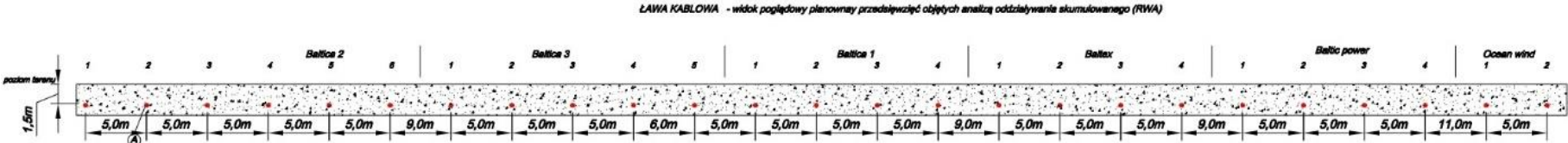


Figure 6.3. The arrangement of individual cable lines in the cable berm as adopted for the modelling of the cumulative magnetic field distribution – RAV

Source: internal data

Table 6.2. *Technical data of the cable berms adopted for the modelling of the magnetic field distribution for individual models [Table 6.1] allowing for the determination of the resultant field distributions, the sources of which are the simultaneously operating cable berms supplying the Baltica-2, Baltica-3, Baltica 1, Baltex, Baltic Power and Ocean Winds end-user stations*

No.	Technical data	Value or description
1	Distance between the centres of symmetry of individual cable berms (all cable trays)	5 m
2	Arrangement of cables in individual cable berms (all cable berms)	Flat
3	The distance between the axes of individual cables in each cable berm	0.3 m
4	Cable diameter (for each cable)	135 mm
5	Cable immersion depth (distance from the earth surface to the cable sheath) – for all cables	1,5 m, and for the Baltic Power cable lines: 2 m
6	Phase arrangement in each cable berm (all cable berms)	Starting from the south: L1 L2 L3 ...L1 L2 L3... L1 L2 L3.....
7	The distances between the cable trays of individual developers	for the APV: - 9 m between B2 and B3; - 11 m between B3 and B1; - 9 m between B1 and Baltex; - 9 m between Baltex and Baltic Power; - 11 m between Baltic Power and Ocean Winds; for the RAV: - 9 m between B2 and B3; - 5 m between B3 and B1; - 9 m between B1 and Baltex; - 9 m between Baltex and Baltic Power; - 11 m between Baltic Power and Ocean Winds
8	The proposed location of the vertical axis in the charts illustrating the magnetic field distributions for each of the models	Halfway between the extreme cables of all cable lines analysed in the model

Source: internal data

Calculations of the cumulative magnetic field distribution for individual variants (APV and RAV) were made by identifying the values of the said quantity at the levels of 0.2, 1.0, and 2.0 m a.g.l., under the recommendation indicated in the regulation (Regulation of the Minister of Climate, Journal of Laws 2020, item 258).

## 6.2 The results of calculations of the magnetic field distribution in the vicinity of the designed common cable berm

The results of calculations of the maximum values of the magnetic field strength (H) that can be expected above the cable berm, in which all cable lines operating simultaneously are located, for both variants, i.e. APV and RAV, are presented in the table below [Table 6.3], while the diagrams of the field intensity distributions magnetic (H) cross-section to the axis of the cable berm is presented in the figures below [Figure 6.4–Figure 6.15].

Table 6.3. Calculation results of the expected maximum values of the magnetic field strength for the analysed models of the cable berm, in which all cable lines supplying subscriber stations Baltica-2, Baltica-3, Baltica 1, Baltex, Baltic Power and Ocean Winds operate simultaneously

Model	Variant (Baltica)	Solution	The maximum expected value of the magnetic field intensity H [ $A \cdot m^{-1}$ ] determined at individual levels [m a.g.l.]		
			0.2	1.0	2.0
M1	APV	Solution 1	20.5	10.1	4.7
M2		Solution 2	27.5	12.6	7.1
M3	RAV	Solution 1	17.5	7.5	4.5
M4		Solution 2	21.9	10.0	5.7

Source: internal data

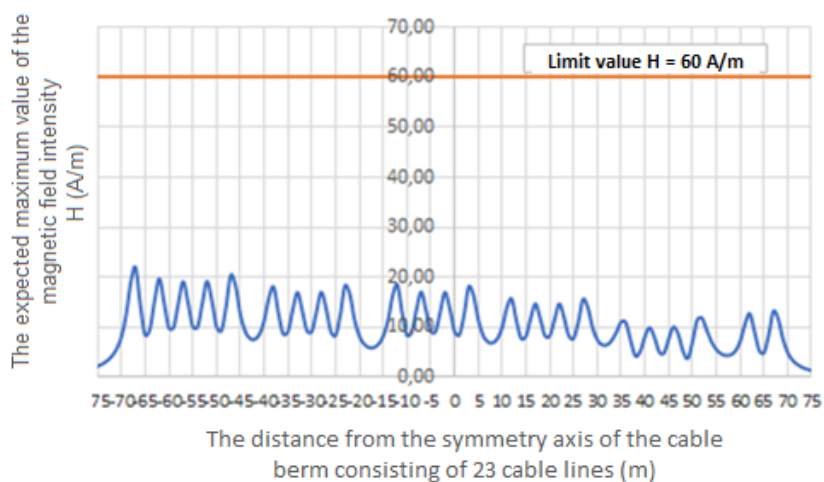


Figure 6.4. The expected maximum value of the magnetic field intensity (H) at a level of 0.2 m a.g.l. as a function of the distance from the axis of the cable berm in which 23 cable lines are run (APV, Solution 1)

Source: internal data

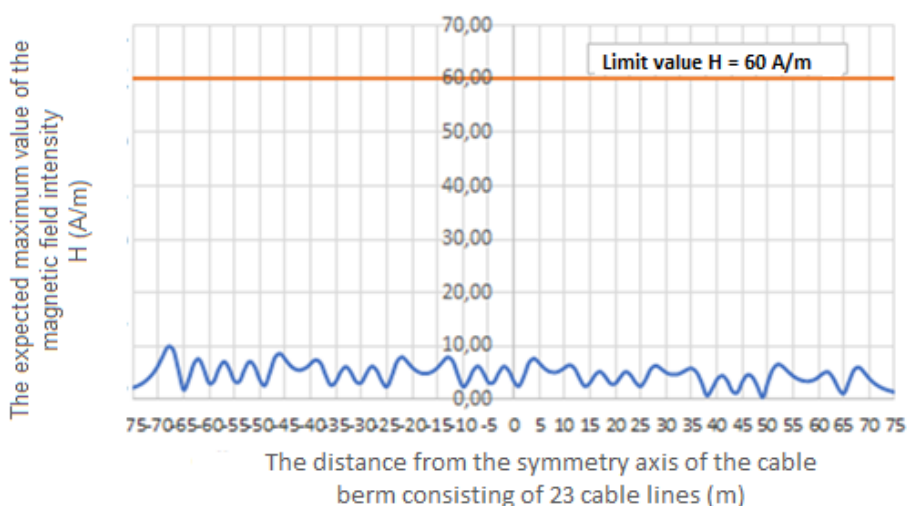


Figure 6.5. The expected maximum value of the magnetic field intensity (H) at a level of 1.0 m a.g.l. as a function of the distance from the axis of the cable berm in which 23 cable lines are run (APV, Solution 1)

Source: internal data

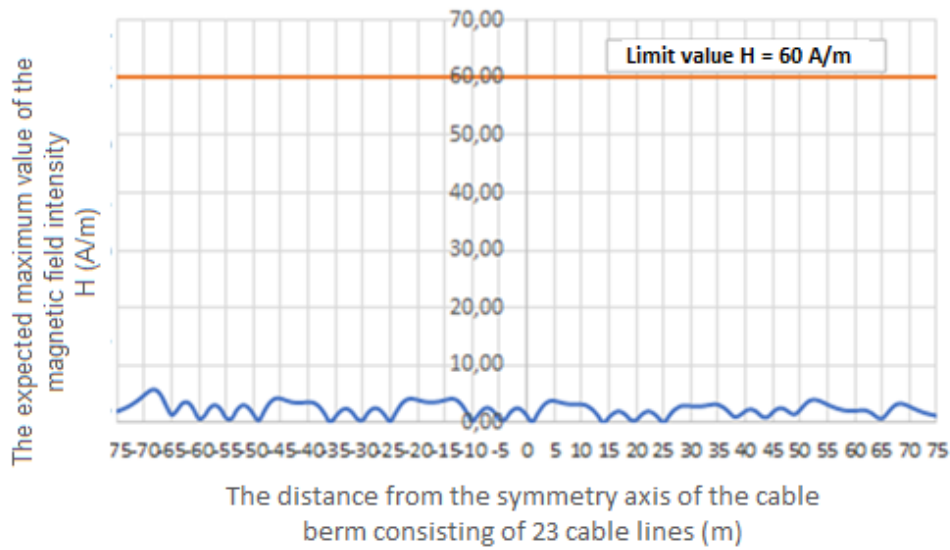


Figure 6.6. The expected maximum value of the magnetic field intensity (H) at a level of 2.0 m a.g.l. as a function of the distance from the axis of the cable berm in which 23 cable lines are run (APV, Solution 1)

Source: internal data

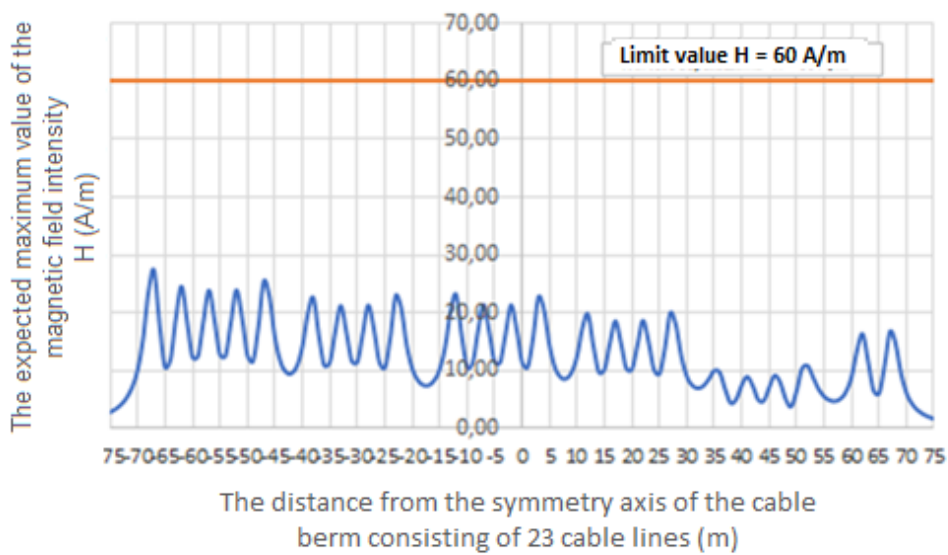


Figure 6.7. The expected maximum value of the magnetic field intensity (H) at a level of 0.2 m a.g.l. as a function of the distance from the axis of the cable berm in which 23 cable lines are run (APV, Solution 2)

Source: internal data

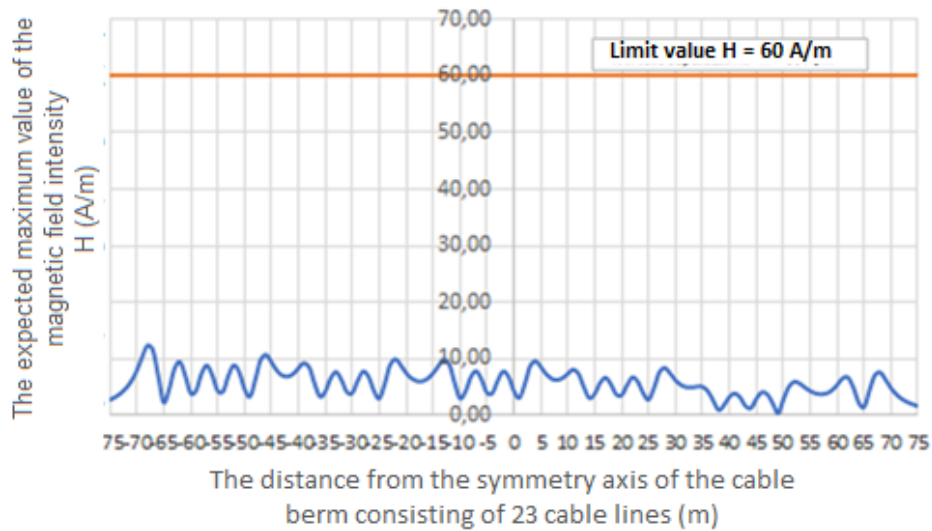


Figure 6.8. The expected maximum value of the magnetic field intensity ( $H$ ) at a level of 1.0 m a.g.l. as a function of the distance from the axis of the cable berm in which 23 cable lines are run (APV, Solution 2)

Source: internal data

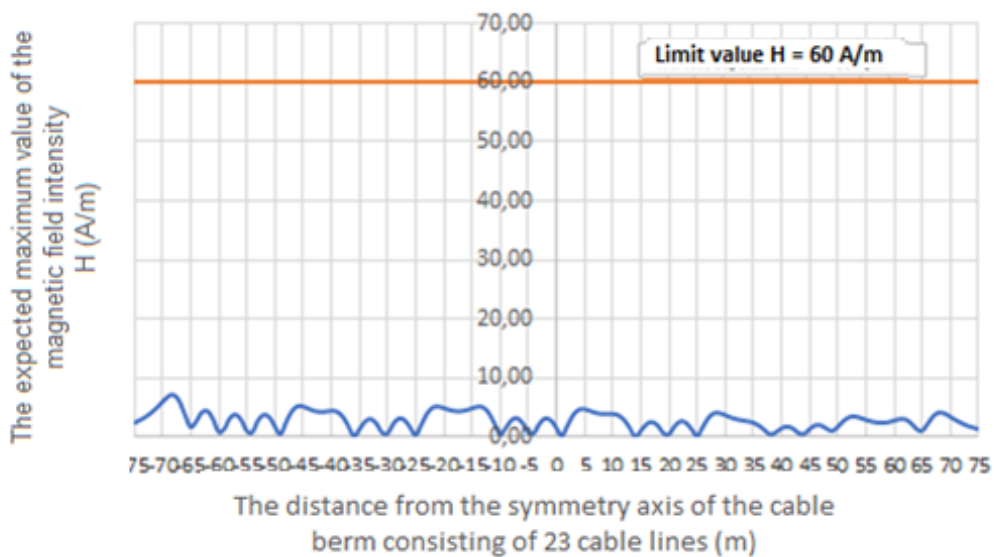


Figure 6.9. The expected maximum value of the magnetic field intensity ( $H$ ) at a level of 2.0 m a.g.l. as a function of the distance from the axis of the cable berm in which 23 cable lines are run (APV, Solution 2)

Source: internal data



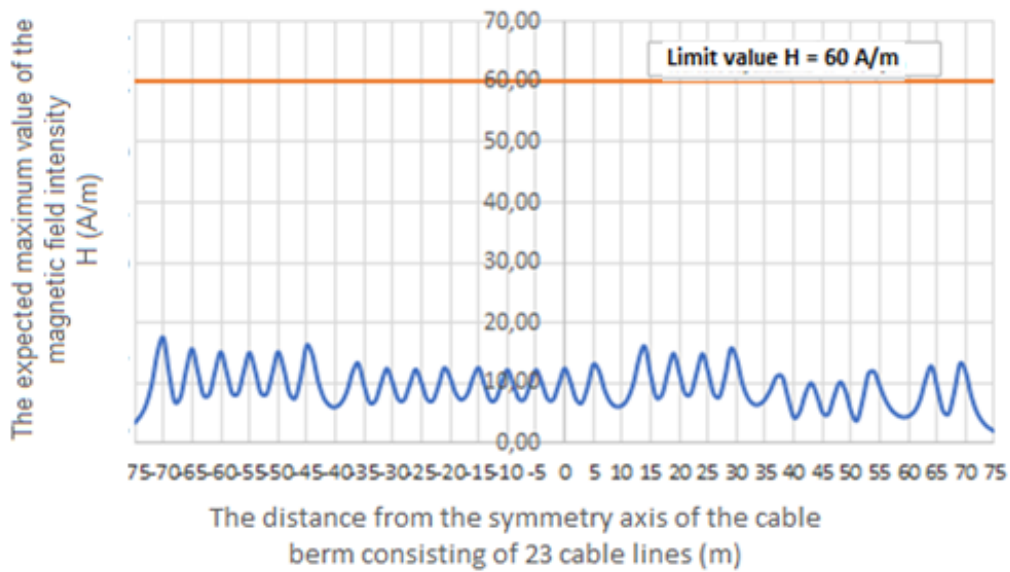


Figure 6.10. The expected maximum value of the magnetic field intensity ( $H$ ) at a level of 0.2 m a.g.l. as a function of the distance from the axis of the cable berm in which 25 cable lines are run (RAV, Solution 1)

Source: internal data

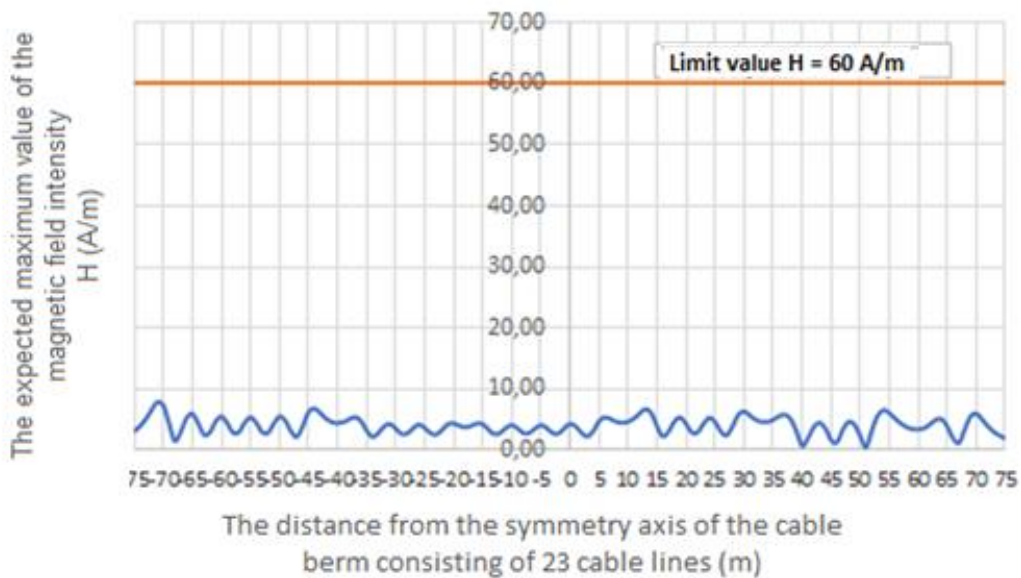


Figure 6.11. The expected maximum value of the magnetic field intensity ( $H$ ) at a level of 1.0 m a.g.l. as a function of the distance from the axis of the cable berm in which 25 cable lines are run (RAV, Solution 1)

Source: internal data

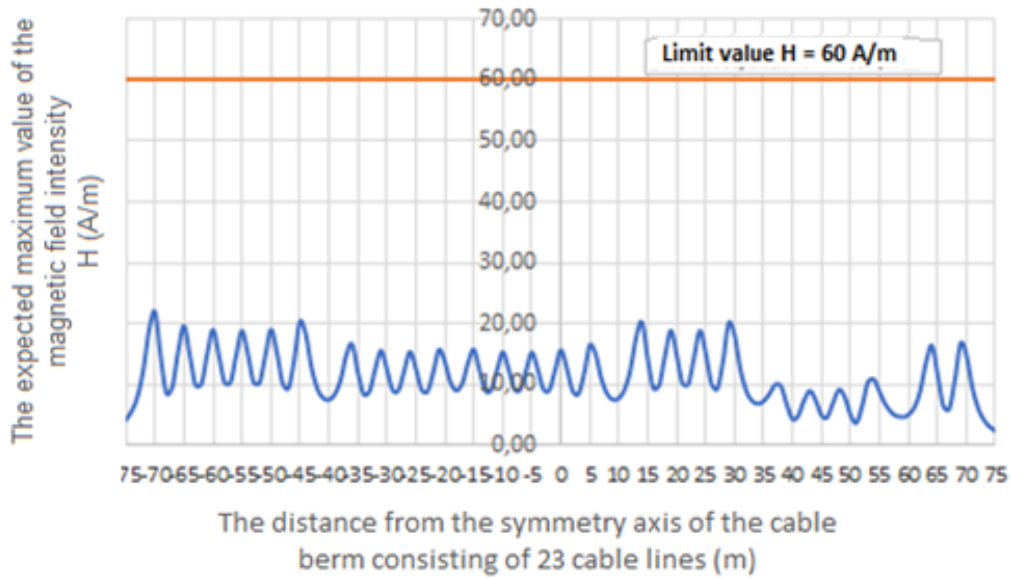


Figure 6.12. The expected maximum value of the magnetic field intensity ( $H$ ) at a level of 2.0 m a.g.l. as a function of the distance from the axis of the cable berm in which 25 cable lines are run (RAV, Solution 1)

Source: internal data

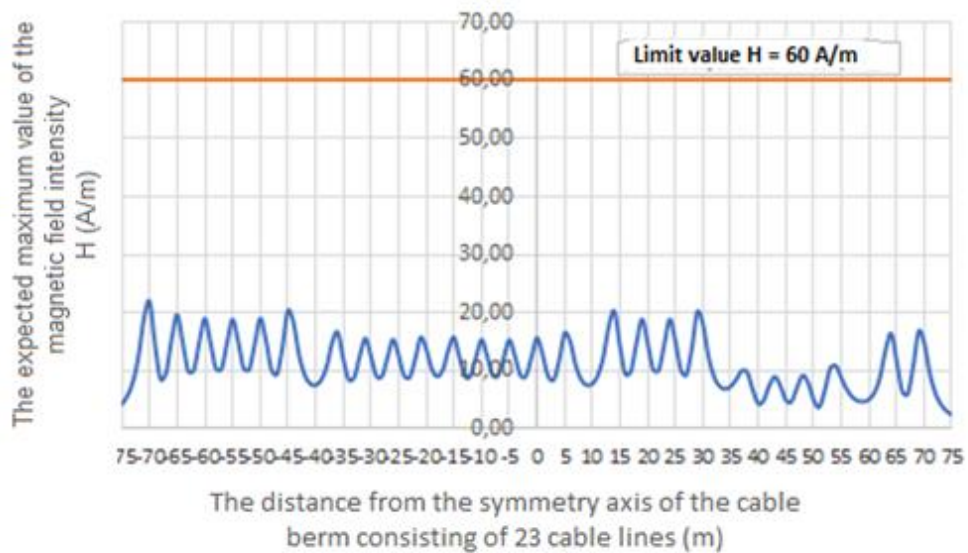


Figure 6.13. The expected maximum value of the magnetic field intensity ( $H$ ) at a level of 0.2 m a.g.l. as a function of the distance from the axis of the cable berm in which 25 cable lines are run (RAV, Solution 2)

Source: internal data

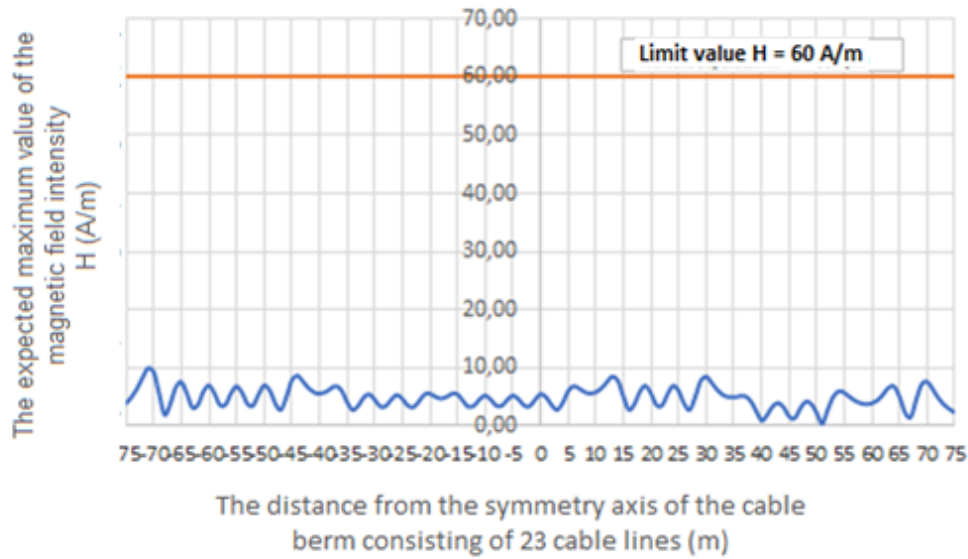


Figure 6.14. The expected maximum value of the magnetic field intensity (H) at a level of 1.0 m a.g.l. as a function of the distance from the axis of the cable berm in which 25 cable lines are run (RAV, Solution 2)

Source: internal data

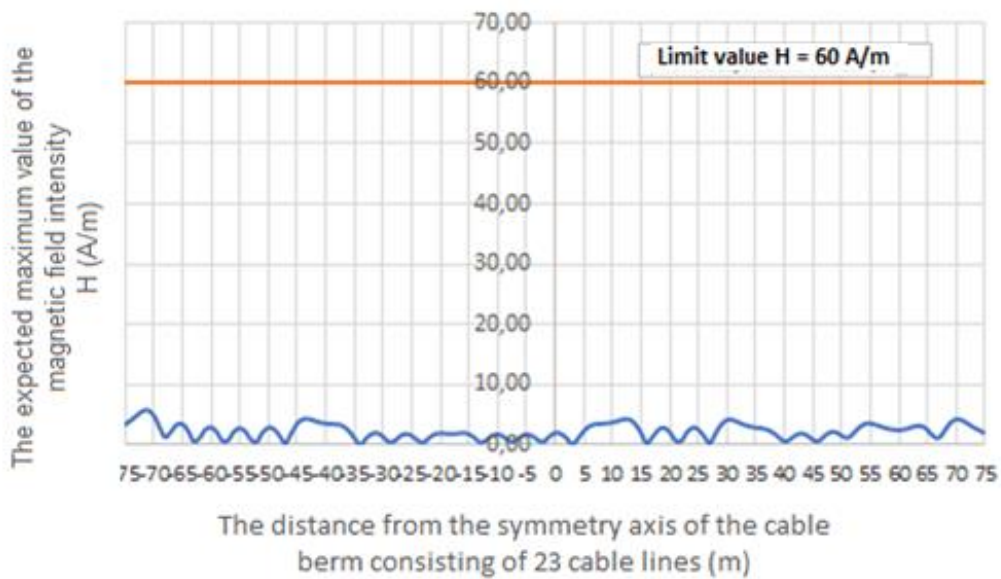


Figure 6.15. The expected maximum value of the magnetic field intensity (H) at a level of 2.0 m a.g.l. as a function of the distance from the axis of the cable berm in which 25 cable lines are run (RAV, Solution 2)

Source: internal data

### 6.3 Interpretation of the results of calculations of the cumulated magnetic field intensity in the vicinity of the cable berm

Calculations of the distribution of the magnetic field (H) generated by cable lines supplying electricity to the designed 6 end-user stations, which form a common cable berm consisting of 23 (APV) or 25 (RAV) cable lines, showed that in none of the analysed cases does the cumulative value of the intensity the magnetic field exceed the permissible value ( $60 \text{ A}\cdot\text{m}^{-1}$ ) established in the regulations applying to places accessible to people. When analysing the expected maximum values of the resultant (cumulative) magnetic field intensity at the levels under consideration (0.2, 1.0 and 2.0 m a.g.l.), it can be noticed that they differ slightly at these levels, regardless of the variant (solution). It is obvious that the highest value of the cumulative magnetic field intensity occurs at a level of 0.2 m a.g.l., due to the shortest distance between the cable lines and the calculation point.

Taking into account the fact that in each of the analysed variants, the cumulative value of the magnetic field intensity is over two times lower than the permissible value ( $60 \text{ A}\cdot\text{m}^{-1}$ ), from the point of view of the potential impact of the magnetic field on the environment, the choice of the analysed solutions may be arbitrary.

## 7 Literature

Raport o oddziaływaniu na środowisko przedsięwzięcia inwestycyjnego pn. „Rozbudowa stacji elektroenergetycznej 220/110 kV Bydgoszcz Zachód wraz z likwidacją kolizji istniejącej linii 220 kV”.

Regulation of the Minister of Climate of 17 February 2020 *on the methods of checking compliance with the permissible levels of electromagnetic fields in the environment*. Journal of Laws 2020, item 258.

Regulation of the Minister of Health of 17 December 2019 *on the permissible levels of electromagnetic fields in the environment*. Journal of Laws 2019, item 2448.

Szuba M., Kowalczyk R., Lenart W., Mikuła J., Szmigielski S., Teresiak Z., Tyszecki A., Linie i stacje elektroenergetyczne w środowisku człowieka. A catalogue. Issue 4. Consulting and Engineering Office “EKO-MARK,” Warsaw 2008.

## 8 List of tables

Table 4.1.	Technical data of the cable berm introducing power from the Baltica OWF into LPSs adopted for the modelling of the EMF distribution .....	11
Table 4.2.	Calculation results of the expected maximum magnetic field intensities in the vicinity of the cable berm for the APV (9 cable lines, flat layout).....	12
Table 4.3.	Calculation results of the expected maximum magnetic field intensities in the vicinity of the cable berm for the RAV (11 cable lines, flat layout).....	13
Table 5.1.	Computation results of the expected maximum intensities of electric (E) and magnetic (H) field in the vicinity of 4 busbars in two-phase configurations (configuration A and B) .....	22
Table 6.1.	Technical data of simultaneously operating power supply systems powering the end-user stations: Baltica 2, Baltica 3, Baltica 1, Baltex, Baltic Power, and Ocean Winds adopted for modelling the distribution of the cumulative magnetic field in the cross-section shown in the figure above [Figure 6.1] .....	27
Table 6.2.	Technical data of the cable berms adopted for the modelling of the magnetic field distribution for individual models [Table 6.1] allowing for the determination of the resultant field distributions, the sources of which are the simultaneously operating cable berms supplying the Baltica-2, Baltica-3, Baltica 1, Baltex, Baltic Power and Ocean Winds end-user stations .....	29
Table 6.3.	Calculation results of the expected maximum values of the magnetic field strength for the analysed models of the cable berm, in which all cable lines supplying subscriber stations Baltica-2, Baltica-3, Baltica 1, Baltex, Baltic Power and Ocean Winds operate simultaneously.....	30

## 9 List of figures

Figure 4.1.	An example of a cross-section of an open trench with 3 single-phase cables with copper or aluminium conductors, constituting a single cable line .....	9
Figure 4.2.	The cross-section of the Baltica OWF CI cable berm (top – APV – 9 cable lines, bottom – RAV – 11 cable lines).....	10
Figure 4.3.	Location of the computation cross-section in which the distribution of the magnetic field intensity was determined .....	12
Figure 4.4.	The expected maximum magnetic field intensity (H) at a level of 0.2 m a.g.l. as a function of the distance from the axis of the cable berm (APV, Solution 1) .....	13
Figure 4.5.	The expected maximum magnetic field intensity (H) at a level of 1.0 m a.g.l. as a function of the distance from the axis of the cable berm (APV, Solution 1) .....	14
Figure 4.6.	The expected maximum magnetic field intensity (H) at a level of 2.0 m a.g.l. as a function of the distance from the axis of the cable berm (APV, Solution 1) .....	14
Figure 4.7.	The expected maximum magnetic field intensity (H) at a level of 0.2 m a.g.l. as a function of the distance from the axis of the cable berm (APV, Solution 2) .....	15
Figure 4.8.	The expected maximum magnetic field intensity (H) at a level of 1.0 m a.g.l. as a function of the distance from the axis of the cable berm (APV, Solution 2) .....	15
Figure 4.9.	The expected maximum magnetic field intensity (H) at a level of 2.0 m a.g.l. as a function of the distance from the axis of the cable berm (APV, Solution 2) .....	16
Figure 4.10.	The expected maximum magnetic field intensity (H) at a level of 0.2 m a.g.l. as a function of the distance from the axis of the cable berm (RAV, Solution 1) .....	16
Figure 4.11.	The expected maximum magnetic field intensity (H) at a level of 1.0 m a.g.l. as a function of the distance from the axis of the cable berm (RAV, Solution 1) .....	17
Figure 4.12.	The expected maximum magnetic field intensity (H) at a level of 2.0 m a.g.l. as a function of the distance from the axis of the cable berm (RAV, Solution 1) .....	17
Figure 4.13.	The expected maximum magnetic field intensity (H) at a level of 0.2 m a.g.l. as a function of the distance from the axis of the cable berm (RAV, Solution 2) .....	18
Figure 4.14.	The expected maximum magnetic field intensity (H) at a level of 1.0 m a.g.l. as a function of the distance from the axis of the cable berm (RAV, Solution 2) .....	18
Figure 4.15.	The expected maximum magnetic field intensity (H) at a level of 2.0 m a.g.l. as a function of the distance from the axis of the cable berm (RAV, Solution 2) .....	19
Figure 5.1.	The location of the busbars evacuating power from the LPSs and the location of the computational cross-section along which the distribution of the electric and magnetic field was determined .....	21
Figure 5.2.	The expected maximum intensity of the electric field (E) at a level of 2.0 m a.g.l. as a function of the distance from the axes of 4 busbars (the axes of symmetry of individual busbars are characterised by the following coordinates: busbar 1: -85 m, busbar 2: -45 m, busbar 3: +45 m, busbar 4: +85 m). The figure below presents the positions of the middle phases (L2) of each busbar (dark blue dots). Phase configuration: A. $10 \text{ kV}\cdot\text{m}^{-1}$ – permissible electric field intensity for places accessible to people.....	22
Figure 5.3.	The expected maximum intensity of the magnetic field (H) at a level of 2.0 m a.g.l. as a function of the distance from the axes of 4 busbars (the axes of symmetry of individual	

busbars are characterised by the following coordinates: busbar 1: -85 m, busbar 2: -45 m, busbar 3: +45 m, busbar 4: +85 m). The figure below presents the positions of the middle phases (L2) of each busbar (dark blue dots). Phase configuration: A ..... 23

Figure 5.4. The expected maximum intensity of the electric field (E) at a level of 2.0 m a.g.l. as a function of the distance from the axes of 4 busbars (the axes of symmetry of individual busbars are characterised by the following coordinates: busbar 1: -85 m, busbar 2: -45 m, busbar 3: +45 m, busbar 4: +85 m). The figure below presents the positions of the middle phases (L2) of each busbar (dark blue dots). Phase configuration: B.  $10 \text{ kV}\cdot\text{m}^{-1}$  – permissible electric field intensity for places accessible to people..... 23

Figure 5.5. The expected maximum intensity of the magnetic field (H) at a level of 2.0 m a.g.l. as a function of the distance from the axes of 4 busbars (the axes of symmetry of individual busbars are characterised by the following coordinates: busbar 1: -85 m, busbar 2: -45 m, busbar 3: +45 m, busbar 4: +85 m). The figure below presents the positions of the middle phases (L2) of each busbar (dark blue dots). Phase configuration: B ..... 24

Figure 6.1. Location of the computational cross-section in which the distribution of the cumulative magnetic field intensity was determined ..... 25

Figure 6.2. The arrangement of individual cable lines in the cable berm as adopted for the modelling of the cumulative magnetic field distribution – APV..... 27

Figure 6.3. The arrangement of individual cable lines in the cable berm as adopted for the modelling of the cumulative magnetic field distribution – RAV..... 28

Figure 6.4. The expected maximum value of the magnetic field intensity (H) at a level of 0.2 m a.g.l. as a function of the distance from the axis of the cable berm in which 23 cable lines are run (APV, Solution 1)..... 30

Figure 6.5. The expected maximum value of the magnetic field intensity (H) at a level of 1.0 m a.g.l. as a function of the distance from the axis of the cable berm in which 23 cable lines are run (APV, Solution 1)..... 30

Figure 6.6. The expected maximum value of the magnetic field intensity (H) at a level of 2.0 m a.g.l. as a function of the distance from the axis of the cable berm in which 23 cable lines are run (APV, Solution 1)..... 31

Figure 6.7. The expected maximum value of the magnetic field intensity (H) at a level of 0.2 m a.g.l. as a function of the distance from the axis of the cable berm in which 23 cable lines are run (APV, Solution 2)..... 31

Figure 6.8. The expected maximum value of the magnetic field intensity (H) at a level of 1.0 m a.g.l. as a function of the distance from the axis of the cable berm in which 23 cable lines are run (APV, Solution 2)..... 32

Figure 6.9. The expected maximum value of the magnetic field intensity (H) at a level of 2.0 m a.g.l. as a function of the distance from the axis of the cable berm in which 23 cable lines are run (APV, Solution 2)..... 32

Figure 6.10. The expected maximum value of the magnetic field intensity (H) at a level of 0.2 m a.g.l. as a function of the distance from the axis of the cable berm in which 25 cable lines are run (RAV, Solution 1) ..... 33

Figure 6.11. The expected maximum value of the magnetic field intensity (H) at a level of 1.0 m a.g.l. as a function of the distance from the axis of the cable berm in which 25 cable lines are run (RAV, Solution 1) ..... 33



Figure 6.12. The expected maximum value of the magnetic field intensity (H) at a level of 2.0 m a.g.l. as a function of the distance from the axis of the cable berm in which 25 cable lines are run (RAV, Solution 1) ..... 34

Figure 6.13. The expected maximum value of the magnetic field intensity (H) at a level of 0.2 m a.g.l. as a function of the distance from the axis of the cable berm in which 25 cable lines are run (RAV, Solution 2) ..... 34

Figure 6.14. The expected maximum value of the magnetic field intensity (H) at a level of 1.0 m a.g.l. as a function of the distance from the axis of the cable berm in which 25 cable lines are run (RAV, Solution 2) ..... 35

Figure 6.15. The expected maximum value of the magnetic field intensity (H) at a level of 2.0 m a.g.l. as a function of the distance from the axis of the cable berm in which 25 cable lines are run (RAV, Solution 2) ..... 35